
Research Article: Confirmation / Disorders of the Nervous System

Rapid onset of motor deficits in a mouse model of spinocerebellar ataxia type 6 precedes late cerebellar degeneration,,

Ataxia onset prior to neurodegeneration in SCA6

Sriram Jayabal, Lovisa Ljungberg, Thomas Erwes, Alexander Cormier, Sabrina Quilez, Sara El Jaouhari and Alanna J. Watt

Department of Biology, McGill University, Montreal, Quebec, Canada.

DOI: 10.1523/ENEURO.0094-15.2015

Received: 17 August 2015

Revised: 4 November 2015

Accepted: 11 November 2015

Published: 4 December 2015

Author Contributions: Research was designed by SJ, TE, LL, and AJW. Behavioral experiments were performed by TE, AC, SJ, SEJ, and SQ, and analyzed by SJ, AC, SQ, and AJW; immunocytochemistry and imaging were performed by LL, SJ, and AJW, and analyzed by LL, SQ, and SJ. Paper was written by SJ and AJW.

Funding: Canadian Institutes of Health Research (CIHR): 130570. Canadian Foundation for Innovation: 29127. Royal Society (UK); McGill University;

Conflict of Interest: The authors declare no competing conflict of interest.

Correspondence should be addressed to: Alanna J. Watt, Department of Biology, McGill University, Bellini Life Sciences Complex, 3649 Sir William Osler, Montreal, QC, H3G 0B1, Canada. Tel: (514) 398-2806. alanna.watt@mcgill.ca

Cite as: eNeuro 2015; 10.1523/ENEURO.0094-15.2015

Alerts: Sign up at eneuro.org/alerts to receive customized email alerts when the fully formatted version of this article is published.

Accepted manuscripts are peer-reviewed but have not been through the copyediting, formatting, or proofreading process.

This is an open-access article distributed under the terms of the Creative Commons Attribution 4.0 International (<http://creativecommons.org/licenses/by/4.0>), which permits unrestricted use, distribution and reproduction in any medium provided that the original work is properly attributed.

Copyright © 2015 Society for Neuroscience

eNeuro

<http://eneuro.msubmit.net>

eN-CFN-0094-15R1

Rapid onset of motor deficits in a mouse model of spinocerebellar ataxia
type 6 precedes late cerebellar degeneration

1. Manuscript Title: Rapid onset of motor deficits in a mouse model of spinocerebellar ataxia type 6 precedes late cerebellar degeneration.

2. Abbreviated Title: Ataxia onset prior to neurodegeneration in SCA6.

3. List of Author Names and Affiliations:

Sriram Jayabal, Lovisa Ljungberg, Thomas Erwes, Alexander Cormier, Sabrina Quilez, Sara El Jaouhari, and Alanna J. Watt*

Department of Biology, McGill University, Montreal, Quebec, Canada.

4. Author Contributions: Research was designed by SJ, TE, LL, and AJW. Behavioral experiments were performed by TE, AC, SJ, SEJ, and SQ, and analyzed by SJ, AC, SQ, and AJW; immunocytochemistry and imaging were performed by LL, SJ, and AJW, and analyzed by LL, SQ, and SJ. Paper was written by SJ and AJW.

5. Correspondence should be addressed to:

Alanna J. Watt

Department of Biology, McGill University

Bellini Life Sciences Complex

3649 Sir William Osler, Montreal, QC, H3G 0B1, Canada

¹alanna.watt@mcgill.ca (514) 398-2806

6. Number of Figures: 8

7. Number of Tables: 2

8. Number of Multimedia: 6

9. Number of words for Abstract: 227

10. Number of words for Significance Statement: 117

11. Number of words for Introduction: 768

12. Number of words for Discussion: 1854

13. Acknowledgements. We thank Jon Sakata for help with statistical analysis, Rüdiger Krahe for the use of his Vibratome, and David Dankort for helpful advice with genotyping. We thank Jesper Sjöström, Anne McKinney, Keith Murai, Visou Ady, Autumn Metzger, Daneck Lang-Ouellette, Corentin Monfort, Adele Tufford, Moushumi Nath, Kevin Liang, and Angela Yang for helpful discussions on this project and/or feedback on the manuscript.

14. Conflict of Interest. The authors declare no competing conflict of interest.

15. Funding Sources. This work was supported by a Canadian Institutes of Health Research (CIHR) Operating Grant (130570), a Canadian Foundation for Innovation (CFI) Leaders' Opportunity Fund (29127), a Royal Society (UK) Equipment Grant, and Start-up funds from McGill University to AJW; it was also supported by a returning IPN (Integrated Program in Neuroscience) student award from McGill University to SJ, and Science Undergraduate Research Awards (SURAs) from McGill University to AC and SQ.

Abstract

Spinocerebellar ataxia type 6 (SCA6) is an autosomal dominant cerebellar ataxia that has been associated with loss of cerebellar Purkinje cells. Disease onset is typically midlife, although it can vary widely from late teens to old age in SCA6 patients. Our study focused on an SCA6 knock-in mouse model with a hyper-expanded (84X) CAG repeat expansion that displays midlife-onset motor deficits at ~7 months old, reminiscent of mid-life onset symptoms in SCA6 patients, although a detailed phenotypic analysis of these mice has not yet been reported. Here, we characterize the onset of motor deficits in SCA6^{84Q} mice using a battery of behavioral assays to test for impairments in motor coordination, balance, and gait. We found that these mice performed normally on these assays up to and including at 6 months, but motor impairment was detected at 7 months with all motor coordination assays used, suggesting that motor deficits emerge rapidly during a narrow age window in SCA6^{84Q} mice. In contrast to what is seen in SCA6 patients, the decrease in motor coordination was observed without alterations in gait. No loss of cerebellar Purkinje cells or striatal neurons were observed at 7 months, the age at which motor deficits were first detected, but significant Purkinje cell loss was observed in 2-year-old SCA6^{84Q} mice, arguing that Purkinje cell death does not significantly contribute to the early stages of SCA6.

Significance Statement

We confirm that disease onset in an 84Q-hyperexpanded polyglutamine mouse model of spinocerebellar ataxia type 6 (SCA6) occurs at 7 months of age, in agreement with a previous study by Watase and colleagues (2008). We characterize disease onset more precisely using a barrage of behavioral tests at multiple ages, and identify that motor coordination abnormalities emerge in a narrow time window between 6 and 7 months, in contrast to the variable age of onset observed in human

Ataxia onset prior to neurodegeneration in SCA6

23 patients. We find that Purkinje cell degeneration occurs in this SCA6 mouse model at 2 years, nearly
24 1.5 years after the onset of motor deficits, demonstrating that Purkinje cell loss is not necessary for
25 early SCA6 disease symptoms.

26 Introduction

27 Spinocerebellar ataxia type 6 (SCA6) is an autosomal dominant neurodegenerative disease that leads to
28 progressive ataxia of the limbs and gait abnormalities, and is one of the most common of the
29 spinocerebellar ataxias (Ashizawa et al., 2013). SCA6 is caused by a CAG-repeat expansion in the gene
30 *CACNA1A* encoding the $\alpha 1A$ -subunit of voltage-dependent P/Q-type calcium channel, causing a
31 polyglutamine (poly-Q) expansion (Zhuchenko et al., 1997). P/Q channels are widely expressed in the
32 brain, including in cerebellar Purkinje cells (Westenbroek et al., 1995; Craig et al., 1998), which
33 undergo degeneration in SCA6 (Yang et al., 2000). In patients, SCA6 symptoms typically present in
34 midlife, with an average onset of ataxic symptoms around ~40-50 years (Matsumura et al., 1997; van
35 de Warrenburg et al., 2002; Ashizawa et al., 2013), although disease onset has been observed across a
36 wide range of ages, from late teens to old age (Yabe et al., 1998).

37 The size of the repeat expansion that gives rise to SCA6 is short compared to other triplet repeat
38 diseases (Gatchel and Zoghbi, 2005): unaffected individuals have <20 repeats, while pathological
39 repeat length is 20-33 (Yabe et al., 1998; van de Warrenburg et al., 2002; Gatchel and Zoghbi, 2005).
40 Consistent with several other triplet-repeat diseases, there is an inverse relationship between CAG
41 repeat expansion length and age of onset in SCA6: longer repeats are correlated with earlier onset of
42 symptoms (Matsumura et al., 1997; van de Warrenburg et al., 2002; Ashizawa et al., 2013). However,
43 the repeat length relationship with the age of disease onset is estimated to account for only 52% of the
44 variance in the age of onset of SCA6 (van de Warrenburg et al., 2002), meaning that individuals who
45 have the same repeat length can differ in the age at which they are first affected by SCA6 by decades.

Ataxia onset prior to neurodegeneration in SCA6

46 We wondered whether similar variability is observed in animal models of SCA6, since this may give
47 insight into the origin of variability of disease onset in human patients.

48 Several mouse models have been developed for SCA6 that show a broadly similar relationship between
49 repeat length and gene dosage on disease onset and severity as observed for human patients, although
50 typically shifted towards longer repeat lengths than those observed in human patients. Mice with
51 human-length triplet repeats (SCA6^{30Q}) have not been observed to develop motor deficiencies (Watase
52 et al., 2008), while a homozygous knock-in mouse model that harbors a hyper-expanded 84-CAG
53 repeat in the encoding region of the P/Q channel subunit (SCA6^{84Q}) displays late-onset motor
54 symptoms similar to human patients: homozygous mice show no motor abnormalities at 3 months but
55 exhibit motor deficits at 7 months (Watase et al., 2008). Furthermore, a mouse with an even longer
56 CAG repeat (SCA6^{118Q}) displays motor impairment as early as 6 weeks old (Unno et al., 2012). While
57 Purkinje cell loss has been reported to rapidly follow motor deficits in the SCA6^{118Q} transgenic mouse
58 (detected at 10 weeks, Unno *et al.*, 2012), no Purkinje cell loss has been reported to date in the late
59 onset SCA6^{84Q} mouse (Watase *et al.*, 2008). More recently, mice overexpressing P/Q-type calcium
60 channel C-terminal fragments containing human-length triplet-repeat insertions have been developed
61 that display motor phenotype (Du et al., 2013; Mark et al., 2015).

62 Since the variable onset of disease symptoms in SCA6 patients is only partially explained by
63 differences in repeat length (van de Warrenburg et al., 2002), we wondered whether variability existed
64 in disease onset in a mouse model of SCA6 as well. Since the SCA6^{84Q} mouse best recapitulates the
65 midlife-onset observed in human SCA6 (Watase et al., 2008), we chose to study the onset of motor
66 coordination symptoms in more detail in the SCA6^{84Q} mouse in order to pinpoint the age of onset of
67 disease symptoms more accurately. We assayed motor coordination of SCA6^{84Q} mice at multiple
68 postnatal ages using several motor coordination assays including Rotarod, elevated beam, and

Ataxia onset prior to neurodegeneration in SCA6

swimming. We found that motor deficits were detected simultaneously with all motor coordination assays, suggesting that there is a narrow and rapid age of onset in this SCA6^{84Q} mouse model, which is strikingly different from the high variability in the age of onset observed in human patients. Motor coordination deficits occurred in 7-month-old mice without any observable difference in gait or changes in Purkinje cell number or morphology, and gait abnormalities were not found even in 2-year-old mice. Although Purkinje cell degeneration was not observed at 7 months in SCA6^{84Q/84Q} mice, these mice have fewer Purkinje cells than WT mice at 2 years, arguing that although Purkinje cell death may contribute to disease progression in SCA6, it does not significantly contribute to early stages of SCA6.

Materials and Methods

Animals. Transgenic SCA6^{84Q} mice were purchased from Jackson Laboratories (strain B6.129S7-*Cacna1atm3Hzo/J*) and heterozygous mice were bred in order to produce litter-matched male and female transgenic SCA6^{84Q} (homozygous, SCA6^{84Q/84Q}, and heterozygous, SCA6^{84Q/+}) and wildtype (WT) mice. At each age, behavioral assays were performed on naive animals with no prior exposure to the assays during a period of 5 consecutive days (see Table 1 for animal numbers at each age), and all data was acquired blind to genotype. Animals were moved from the housing room to the experiment room and allowed 30 min to acclimatize before beginning experiments on each day of testing. Assays were performed in same order: (1) Rotarod, (2) elevated beam assays on days 1–4, (3) swimming; (4) gait was tested last on day (D)5 of testing for 3-7 month-old mice. For 1- and 2-year-old mice, gait was tested first on the first day of testing prior to Rotarod.

Rotarod assay. Animals were placed on a Rotarod (Stoelting Europe, Ireland) using a standard 10-minute long accelerating assay where the rod accelerates from 4-40 RPM in the first 5 minutes and then continues to rotate at 40 RPM for the last 5 minutes (Carter et al., 2001; Watase et al., 2007) (Fig. 1A; Movie 1). The latency to fall was recorded for each mouse as a measure of cerebellar-related motor

Ataxia onset prior to neurodegeneration in SCA6

92 coordination (Watase et al., 2007). Mice performed four trials (T1–4) per day, and had at least a 15 min
93 resting period between trials, over five consecutive days of testing (D1–5).

94 ***Elevated Beam assay.*** Animals walked along a custom-built apparatus consisting of raised round
95 wooden beams (100 cm long), towards a dark escape box as previously described (Carter et al., 2001)
96 (Fig. 2A; Movie 2). Bright light shining on the starting point was used as an aversive stimulus to
97 encourage mice to traverse the beam. D1–2 were training days, during which mice were trained to
98 cross a beam of 22 mm diameter. On days 3 and 4, correspond to testing day 1 and 2, each mouse
99 performed a trial on beams of the following diameters: 22, 18, 15 and 12 mm, totaling to 4 trials per
100 day. The time taken to traverse 80 cm was recorded, and the number of times the mouse's foot slipped
101 while crossing the beams was counted during post-hoc video analysis (see Movie 3 for an example of a
102 mouse whose feet slip 3 times during the assay).

103 ***Swimming assay.*** Animals were trained to swim across a custom-built Plexiglas swimming tank (100
104 cm long by 6 cm wide) towards a dry, boxed-in escape platform (Carter et al., 1999)(Fig. 3A; Movie 3).
105 Bright light at the starting location was used as an aversive stimulus to encourage swimming across the
106 tank. The mice were initially trained to swim across the swim tank towards the escape platform for two
107 trials per day. D1–2 were considered training days, while testing days correspond to D3–5 Mice were
108 videotaped and latency to traverse a 60 cm distance was recorded. The number of hind limb kicks to
109 cross the tank was counted during post-hoc video analysis. After the assay, mice were towel-dried and
110 monitored in their home cage for 20 minutes after the assay.

111 ***Gait Analysis.*** Gait was analyzed as previously described (Carter et al., 2001). The forelimbs and hind
112 limbs of each mouse were coated with distinct colors using non-toxic paint. Mice were prompted to
113 walk across a white sheet affixed to an elevated platform (10 cm high by 10 cm wide) towards a

Ataxia onset prior to neurodegeneration in SCA6

114 custom-built dark escape box (Fig. 4A), leaving a trace of their paw prints on the sheet (Fig. 4B). Stride
115 length (distance between subsequent left and right forelimb and hind limbs; Fig. 5E-F) and stance
116 width (distance between forelimbs and hind limbs; Fig. 5G, H) were measured for 4-6 consecutive
117 strides (measured between the centers of footprints). The co-efficient of variation (CV) between stride
118 lengths as well as the degree of overlap between forelimb and hind limb footprints were recorded from
119 6 consecutive strides. This assay was performed in a single trial on either day 1 (at 1 and 2 years) or
120 day 5 of testing (at 4, 6, and 7 months).

121 **Immunocytochemistry.** Mice were deeply anesthetized and perfused intracardially with 4% PFA (EMS,
122 Hatfield, PA). The brain was extracted and stored in PFA at 4°C for 24 hours, then transferred to PBS
123 with 0.5% sodium azide. The cerebellar vermis was sliced into 100 µm thick parasagittal slices, and the
124 striatum was sliced into 100 µm thick coronal slices on a Leica Vibratome 3000 plus (Concord, ON,
125 Canada). Staining was performed in a blocking solution consisting of 5% BSA, 0.05% sodium azide,
126 and 0.4% Triton X in 0.01 M PBS. The primary antibodies used were rabbit anti-Calbindin D-28k
127 (Swant, Switzerland) at a dilution of 1:1000, and mouse-anti NeuN (Millipore MAB377) tagged with
128 Alexa 488 at a dilution of 1:500, and slices were incubated with this at room temperature on a rotary
129 shaker at 70 RPM for 72 hours. Slices were then rinsed 3X in a solution of 0.4% Triton X in 0.01 M
130 PBS, and for calbindin staining, a secondary antibody (Alexa Fluor 594 anti-rabbit (Jackson
131 ImmunoResearch, West Grove, PA) was used at a dilution of 1:1000 in blocking solution and
132 incubated for 90 minutes at room temperature while shaking. Sections were then rinsed and
133 immediately mounted onto slides with Prolong gold anti-fade mounting solution (Life Technologies,
134 Ontario, Canada) and stored in the dark at 4°C. Slices were imaged with a custom-built two-photon
135 microscope with a Ti:Sapphire laser (MaiTai; SpectraPhysics, Santa Clara, CA) tuned to 775 nm.
136 Image acquisition was done using ScanImage (Pologruto et al., 2003) running in Matlab (Mathworks,

Ataxia onset prior to neurodegeneration in SCA6

137 Natick, MA). Purkinje cell numbers were counted in anterior (lobule 3) or posterior (lobule 9) vermis
 138 as a density per 100 μm Purkinje cell layer, and molecular layer thickness was measured from the
 139 distance between the Purkinje cell layer at multiple evenly-spaced locations in the lobule. Chemicals
 140 were purchased from Sigma unless otherwise indicated.

141 **Data Analysis and statistics.** All data was analyzed blind to genotype. For each behavioral assay,
 142 mouse performance was compared between the three genotypes using one-way ANOVA; when
 143 significance was found, this was followed by Tukey's HSD post-hoc test using JMP Software (SAS,
 144 Cary, NC). Purkinje cell density and molecular layer height were similarly compared with a one-way
 145 ANOVA followed by Tukey's HSD post-hoc test, and imaging data was acquired and analyzed blind to
 146 condition. Striatum cell counts were compared with Student's t-test. Data are reported as mean \pm SEM.

147 **Results**148 ***Rapid onset of motor coordination abnormalities at 7 months old***

149 An accelerating Rotarod assay was used to test the motor coordination of mice at several postnatal ages
 150 ranging from 3 to 7 months (Fig. 1A). The performance of mice on Rotarod was age-dependant, since
 151 younger mice (3 and 4 months old) performed better than older ones (6 months old) on all three
 152 genotypes tested: SCA6^{84Q/84Q}, SCA6^{84Q/+}, and WT (Age: $F_{4, 105} = 10.67$; $P < 0.0001$; Fig. 1B).
 153 Similarly, we found that mice of all genotypes significantly increased their performance across days
 154 within an experimental age (comparing D5 to D1 X Age; $F_{16, 420} = 4.62$; $P < 0.0001$ for 3, 4, 5 and 6
 155 months; Fig. 1B) except at 7 months, where there was no significant increase in performance across
 156 days in any genotype ($P = 0.57$).

157 In agreement with an earlier study by Watase and colleagues (2008), we found that SCA6^{84Q/84Q} mice
 158 exhibited no motor abnormalities at 3 months, but displayed significant motor deficits compared to

Ataxia onset prior to neurodegeneration in SCA6

159 SCA6^{84Q/+} and WT mice at 7 months (Fig. 1B). We wondered if the onset of motor deficits occurred
 160 between these ages, but found no differences in Rotarod performance across genotypes at 4, 5 or 6
 161 months (consult Table 1 for sample size at each age; Fig. 1B), suggesting that the onset of motor
 162 abnormalities in SCA6^{84Q/84Q} mice is not earlier than 7 months, and that disease onset is relatively rapid
 163 between 6 and 7 months old. Since some studies have found that other assays are more sensitive than
 164 Rotarod to detect early motor abnormalities (Stroobants et al., 2013; Lariviere et al., 2015), we chose to
 165 test motor coordination with additional assays as well.

166 We next conducted an elevated beam assay to gain insight into motor coordination and balance in
 167 SCA6^{84Q} mice (Fig. 2A). Using beams of varying diameter, we measured the mice's latency to cross the
 168 beam as an assay of motor coordination. Wide beams are typically easier for mice to walk across than
 169 narrow beams, and we reasoned that a range of beam size might capture subtle motor deficits of fine
 170 motor coordination that were not detectable with Rotarod. In contrast to what we found for Rotarod,
 171 older mice (6 months) performed better by crossing the beams faster than younger mice (3 months) for
 172 all genotypes tested, although this was only true for wide beams (Age: 22 mm beam: $F_{4, 105} = 4.72$; $P =$
 173 0.003 ; 18 mm beam: $F_{4, 105} = 2.36$; $P = 0.04$; Figs. 2B and 2C), while no age-dependence was observed
 174 for narrow diameter beams (15 mm: $P = 0.38$; and 12 mm: $P = 0.14$; Figs. 2D and 2E).

175 SCA6^{84Q/84Q} mice took longer to traverse the elevated beam at 7 months in comparison to WT and
 176 SCA6^{84Q/+} mice for the majority of beams used, while their performance was indistinguishable at
 177 earlier months (Fig. 2B-E). To look in more detail at the elevated beam phenotype, we measured the
 178 number of times each mouse's hind leg feet slipped during beam crossings (Movies 2 and 3). For most
 179 trials, the majority of mice crossed the beam without any footslips irrespective of genotype, age, or
 180 beam width ($P > 0.05$ for all beams and ages excluding 12 mm beam at 7 months; Fig. 3). However, at 7
 181 months, the majority of SCA6^{84Q/84Q} mice experienced footslips when crossing the narrowest beam, and

Ataxia onset prior to neurodegeneration in SCA6

182 this was significantly different from WT or SCA6^{84Q/+} mice (12 mm beam at 7 months: $F_{2,37} = 4.19$; P
183 $= 0.02$; Fig. 3D). Thus, the increased latency to cross most beams for 7-month-old SCA6^{84Q/84Q} mice
184 likely reflects motor coordination and/or balance abnormalities. SCA6^{84Q/+} mice showed no significant
185 differences compared to WT for any age or beam diameter ($P > 0.05$; Fig. 2, 3). In summary, like
186 Rotarod, the elevated beam assay found motor coordination and balance abnormalities in SCA6^{84Q/84Q}
187 mice at 7 months and no earlier, suggesting that the two assays are broadly similar in their ability to
188 detect SCA6 motor abnormalities.

189 While Rotarod and elevated beam are standard assays for motor coordination and balance deficits, we
190 wanted to explore whether less standard motor assays might be useful to detect a motor phenotype in
191 SCA6 mice. Swimming assays have been shown to detect subtle motor deficits at an earlier age than
192 both Rotarod and the elevated beam assay in Huntington's Disease (HD) mice (Carter et al., 1999), and
193 we wondered if this might be similar in SCA6. We used a swimming assay to further characterize
194 motor performance in SCA6^{84Q} mice (Fig. 4A). There were no obvious visual differences in the
195 coordination of the limbs when SCA6^{84Q} mice swam. Unlike with Rotarod and the elevated beam assay,
196 swimming performance showed no age-dependent differences across genotypes at all 5 ages tested, and
197 the latency to cross the tank was not significantly different at any age across genotypes (3, 4, 5, 6, and 7
198 months; Age: $F_{4,104} = 1.13$; $P = 0.35$; Fig. 4B). Mice appear to rely mainly on hind limbs for propulsion
199 through the water when swimming. To determine if there were changes in swimming performance that
200 was not captured by measuring latency, we also counted the number of hind limb swim kicks that were
201 produced to traverse the tank. SCA6^{84Q/+} and WT mice had a similar number of kicks across all ages
202 ($P > 0.05$; Fig. 4C). However, SCA6^{84Q/84Q} mice produced a small but significant increase in hind limb
203 kicks at 7 months on the third day of testing (Fig. 4C, D). These results strengthen our findings from
204 Rotarod and elevated beam assays that SCA6^{84Q/84Q} mice have normal motor ability and coordination

Ataxia onset prior to neurodegeneration in SCA6

up until 6 months, and significant motor deficits are detected one month later at 7 months old, when more hind limb kicks are required to traverse the swim tank.

No gait abnormalities observed in SCA6^{84Q/84Q} mice

Gait abnormalities have been recently reported for presymptomatic SCA6 patients (Rochester et al., 2014), and have also been observed in an SCA6 mouse model with an even longer 118Q expansion repeat (Unno et al., 2012). While no differences in gait were observed by eye, we examined gait in SCA6^{84Q/84Q} mice using foot print analysis (Fig. 5A, B), and found no differences across genotypes for stride length (Fig. 5C–F) or stance width (Fig. 5G, H), and no differences across age 3–7 months for all genotypes (SCA6^{84Q/84Q}, SCA6^{84Q/+}, and WT, $P > 0.05$ for all measurements).

To further test for possible changes in gait, we looked at the variance of stride lengths and paw overlap since stride lengths of mice are known to be very precise with minimal variation (low CV) (Carter et al., 1999). We measured the CV of inter-stride distances from 6 consecutive strides to detect whether changes in this variance could be observed in SCA6^{84Q} mice. We found that the CV of hind limb and forelimb strides was low and not significantly different across genotypes (hind limb stride: Genotype: $F_{2, 63} = 0.27$; $P = 0.77$; forelimb stride: Genotype: $F_{2, 63} = 0.10$; $P = 0.91$; data not shown). We next compared the variance in paw overlap from forelimb and hind limb paws, but found that consistent with our other gait analyses, no significant differences in the CV of inter-paw overlap was observed across genotypes (Genotype: $F_{2, 63} = 0.44$; $P = 0.56$; data not shown). Furthermore, there were no significant age-dependent changes for any genotype ($P > 0.05$ for each measure; refer to table 2). These results suggest that SCA6^{84Q/84Q} mice have normal gait at 7 months despite exhibiting motor coordination deficits that were detected using Rotarod (Fig. 1), elevated beam (Figs. 2 and 3), and swimming assays (Fig. 4).

Ataxia onset prior to neurodegeneration in SCA6

227 We next tested gait in older SCA6^{84Q/84Q} mice to determine if gait abnormalities emerged as the disease
 228 progressed, as has been observed in other mouse models (Unno et al., 2012). Using the same analyses
 229 as we performed at younger ages, we observed a difference comparing 1- and 2-year-old mice on
 230 several gait measurements across genotype (Age: $P < 0.005$ for left and right forelimb and hind limb
 231 stride, left and right stance, and CV of inter-paw overlap; ANOVA followed by post-hoc Tukey's test;
 232 Fig. 6) although not all measures showed significant changes (no significant difference in the CV of
 233 left or right forelimb or hind limb strides, $P > 0.05$; Fig. 6). These data suggest that there is a general
 234 age-related alteration in gait in aging mice. Surprisingly, there were no significant differences in any
 235 measure of gait in 1- or 2-year-old SCA6^{84Q/84Q} mice compared to age-matched WT mice (Fig. 6). This
 236 result strongly argues that gait abnormalities are not observed in SCA6^{84Q/84Q} mice throughout the
 237 majority of their lifespan, although they, like WT mice, experience aging-related gait alterations.

238 To assess disease progression over the same older mice, we examined Rotarod performance in 1- and
 239 2-year-old mice. Motor coordination abnormalities were observed in 1 and 2-year-old SCA6^{84Q/84Q}
 240 mice on Rotarod (Fig. 6), and these deficits progressively worsened compared to deficits observed at 7-
 241 months-old (Age X Genotype $F_{2, 40} = 3.67$; $P = 0.034$; Figs. 1, 6). Taken together, our data illustrate
 242 that motor coordination deficits have a rapid midlife onset in a narrow time window in SCA6^{84Q/84Q}
 243 mice and these symptoms progressively worsen without any alterations in gait.

244 *Late Purkinje cell degeneration in SCA6^{84Q/84Q} mice long after the onset of motor coordination* 245 *deficits*

246 The transgenic SCA6^{84Q/84Q} mice that we use in this study have previously been reported to exhibit no
 247 Purkinje cells degeneration at 20 months old (Watase et al., 2008), which is in contrast to degeneration
 248 observed early in 118Q hyper-expanded mice (Unno et al., 2012) and postmortem in human SCA6

Ataxia onset prior to neurodegeneration in SCA6

249 patient data (Yang et al., 2000). We first examined Purkinje cell density in 7-month-old mice and found
 250 5.2 ± 0.17 cells / 100 μ m Purkinje cell layer in WT mice, with no significant differences in SCA6^{84Q/84Q}
 251 mice (WT: 496 cells measured in 9.7 mm of Purkinje cell layer from N = 3 animals; SCA6^{84Q/84Q}: 490
 252 cells in 9.7 mm of Purkinje cell layer from N = 3 animals; Fig. 7A, B), consistent with previous reports
 253 (Watase et al., 2008). We wondered whether subtle changes in Purkinje cell number or morphology
 254 might be restricted to only part of the cerebellum, since Purkinje cell degeneration has been reported to
 255 be more prevalent in anterior lobules of cerebellar vermis in some human patients (Gierga et al., 2009;
 256 Nanri et al., 2010). To address whether changes might be localised to subregions of cerebellar vermis,
 257 we measured Purkinje cell density in anterior and posterior lobules, but observed no significant
 258 differences in both WT and SCA6^{84Q/84Q} mice (data not shown). To look in more detail at Purkinje cell
 259 morphology at disease onset, we measured the height of the molecular layer (Fig. 7A) as an estimate of
 260 the height of Purkinje cell dendritic trees and found no significant differences between WT and
 261 SCA6^{84Q/84Q} mice at 7 months (WT: 291.8 ± 6.8 μ m; SCA6^{84Q/84Q}: 301.2 ± 8.1 μ m; Fig. 7A, D). Thus,
 262 the onset of disease symptoms in SCA6^{84Q} mice is not associated with alterations in Purkinje cell
 263 number or gross dendritic morphology.

264 Since no changes in Purkinje cell number have been reported in 20-month-old SCA6^{84Q/84Q} mice
 265 (Watase et al., 2008), we looked for degeneration in older mice at 2 years. We observed no significant
 266 reduction in Purkinje cell density in 2-year-old WT mice compared to 7 months, suggesting that little
 267 degeneration has occurred at this age in WT mice ($P = 0.99$; Fig. 7B, D). However, we observed a
 268 reduction in the density of Purkinje cells in SCA6^{84Q/84Q} mice at 2 years compared to 7 months ($P <$
 269 0.0001 ; Fig. 7B, C). Consistent with this, SCA6^{84Q/84Q} mice had ~22% fewer Purkinje cells than their
 270 litter-matched WT siblings at 2 years (WT: 5.09 ± 0.18 cells / 100 μ m, 538 cells measured in 10.3 mm
 271 of Purkinje cell layer from N = 3 mice; SCA6^{84Q/84Q}: 4.01 ± 0.16 cells / 100 μ m, 385 cells in 9.8 mm of

Ataxia onset prior to neurodegeneration in SCA6

272 Purkinje cell layer from N = 3 mice; Fig. 7D). To address whether these changes were localized across
 273 the vermis, we compared the cell density in anterior and posterior lobules in SCA6^{84Q/84Q} mice, and
 274 found no significant differences at 2 years (anterior: 3.7 ± 0.19 cells / 100 μm ; posterior: 4.2 ± 0.25
 275 cells / 100 μm ; $P = 0.51$). Rather, we observed a reduced Purkinje cell density in both anterior and
 276 posterior lobules of SCA6^{84Q/84Q} mice at 2 years compared to age- and litter-matched WT mice
 277 (anterior: $F_{3,92} = 10.16$; $P < 0.0001$; posterior: $F_{3,106} = 3.37$; $P = 0.02$; data not shown), in contrast to
 278 the predominantly anterior Purkinje cell degeneration observed in some human SCA6 patients (Gierga
 279 et al., 2009; Nanri et al., 2010).

280 Since Purkinje cell degeneration has been associated with both a reduction in cell number as well as
 281 structural changes in Purkinje cell dendrites (Yang et al., 2000), we looked at the height of the
 282 molecular layer as a read-out of Purkinje cell dendritic alterations. We found the molecular layer height
 283 in 2-year-old WT mice was 299.5 ± 4.9 μm , which was not significantly different from younger (7
 284 month) WT mice ($P = 0.72$; Fig. 7A,C, D). Together with the cell count data for 2-year-old WT mice
 285 (Fig. 7B), this suggests that very little Purkinje cell degeneration has occurred in the vermis in aged
 286 WT mice. However, the average molecular layer thickness of SCA6^{84Q/84Q} mice at 2 years was $257.8 \pm$
 287 5.3 μm , a ~15% reduction from the molecular layer height in 7-month-old SCA6^{84Q/84Q} mice ($P <$
 288 0.0001). We found that the molecular layer height in 2-year-old SCA6^{84Q/84Q} mice was significantly
 289 reduced compared to age-matched WT mice (Fig. 7C, D). Both our cell count and molecular layer data
 290 suggest that there is significant Purkinje cell degeneration by 2 years in SCA6^{84Q/84Q} mice.

291 Although SCA6 has been considered to be an example of a pure cerebellar ataxia (Solodkin and Gomez,
 292 2012), non-cerebellar symptoms are present in some patients, with up to 25% of affected individuals
 293 having signs of basal ganglia-related symptoms (Solodkin and Gomez, 2012). Since several recent

Ataxia onset prior to neurodegeneration in SCA6

294 studies have reported degeneration in the striatum of patients with other SCAs, including SCA2, SCA3
 295 (Schols et al., 2015), and SCA17 (Brockmann et al., 2012), we looked at the number of striatal neurons
 296 in SCA6^{84Q/84Q} mice at 7 months to determine if degeneration in the striatum was associated with the
 297 onset of motor abnormalities. We found that there were no significant differences between the density
 298 of cells in the striatum of SCA6^{84Q/84Q} and WT mice at 7 months (SCA6^{84Q/84Q}: 1191 ± 36 cells/mm²
 299 striatum, total of 3332 cells counted from N = 4 mice; WT: 1212 ± 48 cells/mm², total of 2586 cells
 300 counted from N = 3 mice; not significantly different, P = 0.72; Fig. 8).

301 Discussion

302 We have performed an in-depth analysis of motor coordination and gait in a late-onset mouse model
 303 (84Q repeat length) of SCA6 in order to better understand the onset and progression of the SCA6
 304 phenotype. We confirm that homozygous SCA6^{84Q/84Q} mice display motor coordination deficits at 7
 305 months, and that deficits were detectable simultaneously in all motor coordination assays tested,
 306 including Rotarod, elevated beam, and swimming. Prior to 7 months, the behavior of SCA6^{84Q/84Q},
 307 SCA6^{84Q/+}, and WT mice were indistinguishable, arguing that motor coordination and performance in
 308 SCA6^{84Q} mice is normal prior to disease onset, and that motor deficits appear rapidly between 6 and 7
 309 months in SCA6^{84Q/84Q} mice. Although Saegusa and colleagues report that heterozygous mice
 310 expressing a human-length (28Q) repeat show enhanced motor coordination compared to WT (Saegusa
 311 et al., 2007), we observe no significant differences between heterozygous SCA6^{84Q/+} and WT mice at
 312 any ages tested, in agreement with previous reports (Watase et al., 2008). In spite of observing motor
 313 coordination deficits in 7-month-old SCA6^{84Q/84Q} mice, we observe no changes in any measures of gait,
 314 suggesting that this mouse model does not reproduce the progression of gait abnormalities typically
 315 observed for the human disease. Indeed, we were unable to detect changes in gait up to 2 years old,
 316 when motor coordination deficits had worsened, arguing that gait and motor coordination deficits can

Ataxia onset prior to neurodegeneration in SCA6

317 present independently. Finally, the onset of disease symptoms in SCA6 is not accompanied by
 318 morphological changes or survival of cerebellar Purkinje cells, although Purkinje cell degeneration,
 319 reflecting both reductions in dendritic height and cell number, is observed nearly 1.5 years later in 2-
 320 year-old SCA6^{84Q/84Q} mice. The long time delay between disease onset and Purkinje cell degeneration
 321 suggests that Purkinje cell loss does not significantly contribute to early stages of SCA6
 322 pathophysiology, and suggests that the potential for therapeutic intervention before cell death occurs
 323 might be a promising avenue of future study.

324 *Comparison of motor assays for detection of SCA6 and motor abnormalities*

325 We studied a range of motor coordination assays in SCA6^{84Q} mice as it was unknown if one motor
 326 assay would be more sensitive than others to subtle changes in motor coordination in SCA6. With
 327 Rotarod, a mouse has the opportunity to slip only one time per trial, upon which it typically falls, which
 328 means that graded differences in motor performance may be underestimated. We reasoned that other
 329 motor coordination assays, like the elevated beam in which mice can slip multiple times during the
 330 completion of the task, might provide a more nuanced read-out of motor deficits, as has been observed
 331 in some animal models of ataxia (Lariviere et al., 2015), although there are animal models, like the
 332 SCA3 transgenic mouse, where deficits are detected with Rotarod before elevated beam (Switonski et
 333 al., 2015). We also used a swimming assay which has been shown to detect motor abnormalities in a
 334 HD transgenic mouse earlier than the elevated beam (Carter et al., 1999). Since we observe similar
 335 results with 3 different motor coordination assays, we argue that these assays have comparable power
 336 to detect motor coordination deficit onset in SCA6. However, in our hands Rotarod is simpler and
 337 easier to administer than the elevated beam or swimming assays, making it our preferred assay for
 338 SCA6 detection. It is possible, however, that even more sensitive assays exist to detect SCA6 motor
 339 abnormalities in rodents that we have not tested (e.g. (Vinueza Veloz et al., 2014; Jarrahi et al., 2015)).

Ataxia onset prior to neurodegeneration in SCA6

340 We found robust motor deficits at 7 months without any concomitant changes in gait, and indeed gait
341 abnormalities were not observed even in 2-year-old SCA6^{84Q/84Q} mice. This may at first appear
342 surprising given that gait abnormalities are some of the first changes to be observed in SCA6 patients
343 (Rochester et al., 2014), and gait abnormalities have been observed in an SCA6 mouse model with an
344 even longer poly-Q expansion repeat (Unno et al., 2012). However, although motor coordination
345 deficits and gait abnormalities often present together in mouse models (e.g. (Chen et al., 2015;
346 Swarnkar et al., 2015)), this is not always the case: there are some ataxic models where gait
347 abnormalities and motor coordination deficits are not temporally correlated (e.g. (Clark et al., 1997;
348 Simon et al., 2004; Lariviere et al., 2015)), while in other transgenic mouse models, gait abnormalities
349 have even been shown to accompany enhanced performance on motor coordination assays (Nakatani et
350 al., 2009; Piochon et al., 2014). The absence of gait abnormalities with motor coordination changes in
351 SCA6^{84Q/84Q} mice highlights a limitation of this model to faithfully recapitulate human SCA6
352 symptoms (Rochester et al., 2014).

353 In addition to the reduced motor coordination observed with each motor assay for SCA6^{84Q/84Q} mice at
354 7 months, we also observed age-dependent changes in performance across genotypes that were
355 strikingly different for the different motor assays we used: Rotarod showed *decreased* motor
356 performance with age, the elevated beam assay showed *increased* motor performance with age for
357 wider beams, while swimming showed no apparent age-related differences in performance. While we
358 and others have found decreased Rotarod performance in aged WT mice (>18 months for (Barreto et al.,
359 2010); 2 years, Fig. 6D), which has been posited to arise because of neurodegeneration, we saw no
360 significant reduction in WT Purkinje cell density at 2 years compared to 7 months (Fig. 7). In any case,
361 degeneration cannot explain the age-dependent decreases in performance seen in 7-month-old mice of
362 all genotypes with Rotarod (Fig. 1). All 3 genotypes showed reduced performance with Rotarod at 7

Ataxia onset prior to neurodegeneration in SCA6

363 months compared to earlier performance; this suggests that there is a natural decline in performance
 364 around 7 months that is exacerbated in SCA6^{84Q/84Q} mice. Understanding the mechanism of aging-
 365 dependent decline at 7 months in all genotypes may provide insight into disease onset in SCA6.

366 Another difference between Rotarod and the elevated beam assay is that for a given age, performance
 367 tends to improve on successive trials per day (data not shown) as well as over experimental days with
 368 Rotarod (Fig. 1), while on the elevated beam mice tend to perform worse on the second day of training
 369 on most beam diameters (Fig. 2). In our experience, this day-on-day declining performance reflects at
 370 least in part the mice's waning motivation to cross the beam, which could confound the evaluation of
 371 motor coordination with this assay, while the day-on-day improvement observed with Rotarod may
 372 involve cerebellar learning (Ly et al., 2013). For the swimming assay, there is little day-on-day or age-
 373 dependent changes in performance, suggesting that this assay may not be best suited to measure some
 374 aspects of motor performance. For these reasons we find that Rotarod is our best assay to detect motor
 375 learning alterations in mouse models of SCA6.

376 *Implications of SCA6^{84Q} Mouse model for human SCA6*

377 While motor coordination abnormalities have been observed in SCA6^{84Q/84Q} mice at 7 months in a
 378 previous study (Watase et al., 2008), since only a few time points were studied with a single motor
 379 assay in this previous report, the onset of disease symptoms was not well understood. Here we have
 380 characterized a rapid disease onset between 6 and 7 months that is detected with multiple behavioural
 381 assays, suggesting that disease onset is relatively strong since it can be detected by assays of varying
 382 sensitivity. This characterization of SCA6^{84Q/84Q} mice helps to strengthen this transgenic mouse as a
 383 model system for studying disease onset in SCA6. Our result of a narrow age of onset of disease
 384 symptoms is in contrast to observations in human patients, where individuals with a given repeat length

Ataxia onset prior to neurodegeneration in SCA6

385 can differ in age of onset by decades (van de Warrenburg et al., 2002). What might account for the
 386 discrepancy in disease onset variability between human patients and this transgenic mouse model?
 387 Transgenic SCA6^{84Q} mice are genetically homologous and live in a controlled environment, thus both
 388 genetic and environmental diversity that exists in SCA6 patients may be absent in our study. Future
 389 enquiry is required into understanding the contribution of epigenetic, environmental, and/or epistatic
 390 influences on SCA6 disease onset.

391 Since Purkinje cell loss is a common attribute of SCA6 (Yang et al., 2000), one of the limitations of the
 392 SCA6^{84Q} transgenic mouse model in the past has been the absence of reported Purkinje cell
 393 degeneration (Watase et al., 2008), unlike in other mouse models where Purkinje cell death is detected
 394 within weeks of disease onset (Unno et al., 2012). We observe Purkinje cell degeneration in 2-year-old
 395 SCA6^{84Q/84Q} mice, nearly 1.5 years after the onset of motor deficits, which argues that Purkinje cell
 396 death does not contribute to early onset of motor abnormalities, and supports findings from other SCA6
 397 mouse models suggesting that early symptoms of SCA6 arise from cellular alterations. Mechanisms
 398 that might contribute to the onset of motor dysfunction might be cellular inclusions in Purkinje cells
 399 (Watase et al., 2008; Mark et al., 2015), although Watase and colleagues show immunocytochemical
 400 evidence for these inclusions only at later ages (22 months), long after the onset of motor dysfunction
 401 in these mice (Watase et al., 2008). Other mechanisms contributing to early motor dysfunction might
 402 be due to a C-terminal fragment encoded by the *CACNA1A* gene that may act as a transcription factor
 403 (Du et al., 2013), and/or may have deleterious action in the cytoplasm of Purkinje cells (Mark et al.,
 404 2015). Changes in synaptic input to Purkinje cells may also be involved (Mark et al., 2015). Our
 405 demonstration of Purkinje cell degeneration, a key feature of human SCA6 (Yang et al., 2000), in aged
 406 SCA6^{84Q/84Q} mice supports these mice as a good model system of SCA6. From a therapeutic
 407 perspective, these results are promising, as they suggest a window for therapeutic intervention might

Ataxia onset prior to neurodegeneration in SCA6

408 exist where motor function could be ameliorated by the rescue of cellular abnormalities before cell
409 death occurs. Rescue of motor function after cell death at later stages of the disease may be more
410 challenging, and may require different therapeutic approaches.

411 Several recent studies on SCAs have found that neural degeneration is not limited to cerebellum. For
412 instance, degeneration of neurons in the striatum has been observed in SCA2, SCA3 (Schols et al.,
413 2015), and SCA17 (Brockmann et al., 2012). Interestingly, significant degeneration has been observed
414 in the striatum without motor symptoms in both HD (Cowan and Raymond, 2006), and in several SCAs
415 (Brockmann et al., 2012; Schols et al., 2015), which made us wonder whether changes in the striatum
416 might be involved in the onset of motor symptoms in SCA6. However, we found no significant cell
417 loss in the stratum of SCA6^{84Q/84Q} mice at 7 months, suggesting that striatal degeneration is unlikely to
418 contribute to early stages of disease onset in SCA6.

419 In summary, homozygous SCA6^{84Q/84Q} mice display motor coordination deficits that arise rapidly
420 between 6 and 7 months without gait abnormalities or Purkinje cell degeneration. Motor coordination
421 deficits progress, and Purkinje cell degeneration is observed in 2-year-old SCA6^{84Q/84Q} mice,
422 confirming that these mice display this hallmark feature of human SCA6. The temporal lag between
423 disease onset and neuronal degeneration argues that degeneration plays a role only in later stages of
424 SCA6. These results are important as they suggest that a wide therapeutic window may exist after
425 SCA6 disease onset before cell death occurs.

426 References

427 Ashizawa T et al. (2013) Clinical characteristics of patients with spinocerebellar ataxias 1, 2, 3 and 6 in
428 the US; a prospective observational study. Orphanet J Rare Dis 8:177.

Ataxia onset prior to neurodegeneration in SCA6

- 429 Barreto G, Huang TT, Giffard RG (2010) Age-related defects in sensorimotor activity, spatial learning,
430 and memory in C57BL/6 mice. *J Neurosurg Anesthesiol* 22:214-219.
- 431 Brockmann K, Reimold M, Globas C, Hauser TK, Walter U, Machulla HJ, Rolfs A, Schols L (2012)
432 PET and MRI reveal early evidence of neurodegeneration in spinocerebellar ataxia type 17. *J Nucl Med*
433 53:1074-1080.
- 434 Carter RJ, Morton J, Dunnett SB (2001) Motor coordination and balance in rodents. *Curr Protoc*
435 *Neurosci* Chapter 8:Unit 8 12.
- 436 Carter RJ, Lione LA, Humby T, Mangiarini L, Mahal A, Bates GP, Dunnett SB, Morton AJ (1999)
437 Characterization of progressive motor deficits in mice transgenic for the human Huntington's disease
438 mutation. *J Neurosci* 19:3248-3257.
- 439 Chen ZZ, Wang CM, Lee GC, Hsu HC, Wu TL, Lin CW, Ma CK, Lee-Chen GJ, Huang HJ, Hsieh-Li
440 HM (2015) Trehalose attenuates the gait ataxia and gliosis of spinocerebellar ataxia type 17 mice.
441 *Neurochem Res* 40:800-810.
- 442 Clark HB, Burright EN, Yunis WS, Larson S, Wilcox C, Hartman B, Matilla A, Zoghbi HY, Orr HT
443 (1997) Purkinje cell expression of a mutant allele of SCA1 in transgenic mice leads to disparate effects
444 on motor behaviors, followed by a progressive cerebellar dysfunction and histological alterations. *J*
445 *Neurosci* 17:7385-7395.

Ataxia onset prior to neurodegeneration in SCA6

- 446 Cowan CM, Raymond LA (2006) Selective neuronal degeneration in Huntington's disease. *Curr Top*
- 447 *Dev Biol* 75:25-71.
- 448 Craig PJ, McAinsh AD, McCormack AL, Smith W, Beattie RE, Priestley JV, Yip JL, Averill S,
- 449 Longbottom ER, Volsen SG (1998) Distribution of the voltage-dependent calcium channel α 1A
- 450 subunit throughout the mature rat brain and its relationship to neurotransmitter pathways. *The Journal*
- 451 *of comparative neurology* 397:251-267.
- 452 Du X, Wang J, Zhu H, Rinaldo L, Lamar KM, Palmenberg AC, Hansel C, Gomez CM (2013) Second
- 453 cistron in CACNA1A gene encodes a transcription factor mediating cerebellar development and SCA6.
- 454 *Cell* 154:118-133.
- 455 Gatchel JR, Zoghbi HY (2005) Diseases of unstable repeat expansion: mechanisms and common
- 456 principles. *Nat Rev Genet* 6:743-755.
- 457 Gierga K, Schelhaas HJ, Brunt ER, Seidel K, Scherzed W, Egensperger R, de Vos RA, den Dunnen W,
- 458 Ippel PF, Petrasch-Parwez E, Deller T, Schols L, Rub U (2009) Spinocerebellar ataxia type 6 (SCA6):
- 459 neurodegeneration goes beyond the known brain predilection sites. *Neuropathol Appl Neurobiol*
- 460 35:515-527.
- 461 Jarrahi M, Sedighi Moghadam B, Torkmandi H (2015) An experimental evaluation of a new designed
- 462 apparatus (NDA) for the rapid measurement of impaired motor function in rats. *J Neurosci Methods*
- 463 251:138-142.

Ataxia onset prior to neurodegeneration in SCA6

- 464 Lariviere R, Gaudet R, Gentil BJ, Girard M, Conte TC, Minotti S, Leclerc-Desaulniers K, Gehring K,
465 McKinney RA, Shoubridge EA, McPherson PS, Durham HD, Brais B (2015) Sacs knockout mice
466 present pathophysiological defects underlying autosomal recessive spastic ataxia of Charlevoix-
467 Saguenay. *Hum Mol Genet* 24:727-739.
- 468 Ly R, Bouvier G, Schonewille M, Arabo A, Rondi-Reig L, Lena C, Casado M, De Zeeuw CI, Feltz A
469 (2013) T-type channel blockade impairs long-term potentiation at the parallel fiber-Purkinje cell
470 synapse and cerebellar learning. *Proc Natl Acad Sci U S A* 110:20302-20307.
- 471 Mark MD, Krause M, Boele HJ, Kruse W, Pollok S, Kuner T, Dalkara D, Koekkoek S, De Zeeuw CI,
472 Herlitze S (2015) Spinocerebellar Ataxia Type 6 Protein Aggregates Cause Deficits in Motor Learning
473 and Cerebellar Plasticity. *J Neurosci* 35:8882-8895.
- 474 Matsumura R, Futamura N, Fujimoto Y, Yanagimoto S, Horikawa H, Suzumura A, Takayanagi T
475 (1997) Spinocerebellar ataxia type 6. Molecular and clinical features of 35 Japanese patients including
476 one homozygous for the CAG repeat expansion. *Neurology* 49:1238-1243.
- 477 Nakatani J, Tamada K, Hatanaka F, Ise S, Ohta H, Inoue K, Tomonaga S, Watanabe Y, Chung YJ,
478 Banerjee R, Iwamoto K, Kato T, Okazawa M, Yamauchi K, Tanda K, Takao K, Miyakawa T, Bradley
479 A, Takumi T (2009) Abnormal behavior in a chromosome-engineered mouse model for human 15q11-
480 13 duplication seen in autism. *Cell* 137:1235-1246.

Ataxia onset prior to neurodegeneration in SCA6

- 481 Nanri K, Koizumi K, Mitoma H, Taguchi T, Takeguchi M, Ishiko T, Otsuka T, Nishioka H, Mizusawa
- 482 H (2010) Classification of cerebellar atrophy using voxel-based morphometry and SPECT with an easy
- 483 Z-score imaging system. Intern Med 49:535-541.
- 484 Piochon C, Kloth AD, Grasselli G, Titley HK, Nakayama H, Hashimoto K, Wan V, Simmons DH,
- 485 Eissa T, Nakatani J, Cherskov A, Miyazaki T, Watanabe M, Takumi T, Kano M, Wang SS, Hansel C
- 486 (2014) Cerebellar plasticity and motor learning deficits in a copy-number variation mouse model of
- 487 autism. Nat Commun 5:5586.
- 488 Pologruto TA, Sabatini BL, Svoboda K (2003) ScanImage: flexible software for operating laser
- 489 scanning microscopes. Biomed Eng Online 2:13.
- 490 Rochester L, Galna B, Lord S, Mhiripiri D, Eglon G, Chinnery PF (2014) Gait impairment precedes
- 491 clinical symptoms in spinocerebellar ataxia type 6. Mov Disord 29:252-255.
- 492 Saegusa H, Wakamori M, Matsuda Y, Wang J, Mori Y, Zong S, Tanabe T (2007) Properties of human
- 493 Cav2.1 channel with a spinocerebellar ataxia type 6 mutation expressed in Purkinje cells. Molecular
- 494 and cellular neurosciences 34:261-270.
- 495 Schols L, Reimold M, Seidel K, Globas C, Brockmann K, Karsten Hauser T, Auburger G, Burk K, den
- 496 Dunnen W, Reischl G, Korf HW, Brunt ER, Rub U (2015) No parkinsonism in SCA2 and SCA3
- 497 despite severe neurodegeneration of the dopaminergic substantia nigra. Brain.

Ataxia onset prior to neurodegeneration in SCA6

- 498 Simon D, Seznec H, Gansmuller A, Carelle N, Weber P, Metzger D, Rustin P, Koenig M, Puccio H
 499 (2004) Friedreich ataxia mouse models with progressive cerebellar and sensory ataxia reveal
 500 autophagic neurodegeneration in dorsal root ganglia. *J Neurosci* 24:1987-1995.
- 501 Solodkin A, Gomez CM (2012) Spinocerebellar ataxia type 6. *Handb Clin Neurol* 103:461-473.
- 502 Stroobants S, Gantois I, Pooters T, D'Hooge R (2013) Increased gait variability in mice with small
 503 cerebellar cortex lesions and normal rotarod performance. *Behav Brain Res* 241:32-37.
- 504 Swarnkar S, Chen Y, Pryor WM, Shahani N, Page DT, Subramaniam S (2015) Ectopic expression of
 505 the striatal-enriched GTPase Rhes elicits cerebellar degeneration and an ataxia phenotype in
 506 Huntington's disease. *Neurobiol Dis* 82:66-77.
- 507 Switonski PM, Szlachcic WJ, Krzyzosiak WJ, Figiel M (2015) A new humanized ataxin-3 knock-in
 508 mouse model combines the genetic features, pathogenesis of neurons and glia and late disease onset of
 509 SCA3/MJD. *Neurobiol Dis* 73:174-188.
- 510 Unno T, Wakamori M, Koike M, Uchiyama Y, Ishikawa K, Kubota H, Yoshida T, Sasakawa H, Peters
 511 C, Mizusawa H, Watase K (2012) Development of Purkinje cell degeneration in a knockin mouse
 512 model reveals lysosomal involvement in the pathogenesis of SCA6. *Proc Natl Acad Sci U S A*
 513 109:17693-17698.

Ataxia onset prior to neurodegeneration in SCA6

- 514 van de Warrenburg BP, Sinke RJ, Verschuuren-Bemelmans CC, Scheffer H, Brunt ER, Ippel PF, Maat-
515 Kievit JA, Dooijes D, Notermans NC, Lindhout D, Knoers NV, Kremer HP (2002) Spinocerebellar
516 ataxias in the Netherlands: prevalence and age at onset variance analysis. *Neurology* 58:702-708.
- 517 Vinueza Veloz MF, Zhou K, Bosman LW, Potters JW, Negrello M, Seepers RM, Strydis C, Koekkoek
518 SK, De Zeeuw CI (2014) Cerebellar control of gait and interlimb coordination. *Brain Struct Funct*.
- 519 Watase K, Gatchel JR, Sun Y, Emamian E, Atkinson R, Richman R, Mizusawa H, Orr HT, Shaw C,
520 Zoghbi HY (2007) Lithium therapy improves neurological function and hippocampal dendritic
521 arborization in a spinocerebellar ataxia type 1 mouse model. *PLoS Med* 4:e182.
- 522 Watase K, Barrett CF, Miyazaki T, Ishiguro T, Ishikawa K, Hu Y, Unno T, Sun Y, Kasai S, Watanabe
523 M, Gomez CM, Mizusawa H, Tsien RW, Zoghbi HY (2008) Spinocerebellar ataxia type 6 knockin
524 mice develop a progressive neuronal dysfunction with age-dependent accumulation of mutant CaV2.1
525 channels. *Proc Natl Acad Sci U S A* 105:11987-11992.
- 526 Westenbroek RE, Sakurai T, Elliott EM, Hell JW, Starr TV, Snutch TP, Catterall WA (1995)
527 Immunochemical identification and subcellular distribution of the alpha 1A subunits of brain calcium
528 channels. *J Neurosci* 15:6403-6418.
- 529 Yabe I, Sasaki H, Yamashita I, Takei A, Fukazawa T, Hamada T, Tashiro K (1998) [Initial symptoms
530 and mode of neurological progression in spinocerebellar ataxia type 6 (SCA6)]. *Rinsho shinkeigaku =*
531 *Clinical neurology* 38:489-494.

Ataxia onset prior to neurodegeneration in SCA6

532 Yang Q, Hashizume Y, Yoshida M, Wang Y, Goto Y, Mitsuma N, Ishikawa K, Mizusawa H (2000)
533 Morphological Purkinje cell changes in spinocerebellar ataxia type 6. *Acta neuropathologica* 100:371-
534 376.

535 Zhuchenko O, Bailey J, Bonnen P, Ashizawa T, Stockton DW, Amos C, Dobyns WB, Subramony SH,
536 Zoghbi HY, Lee CC (1997) Autosomal dominant cerebellar ataxia (SCA6) associated with small
537 polyglutamine expansions in the α 1A-voltage-dependent calcium channel. *Nat Genet* 15:62-69.

538

539

540 **Legends**

541 **Figure 1. Rotarod deficits at 7 months in SCA6^{84Q/84Q} mice.**

542 A, schematic of experimental paradigm: accelerating Rotarod experiments were conducted for 4
 543 trials/day for 5 days of testing at each age. B, no significant differences on D4–5 were observed
 544 between SCA6^{84Q/84Q}, SCA6^{84Q/+}, and WT genotypes at 3, 4, 5 or 6 months old; however, SCA6^{84Q/84Q}
 545 mice display poorer performance on Rotarod on D4–5 at 7 months compared to WT mice (Genotype:
 546 $F_{2,37} = 12.19$; $P = 0.0004$, one-way ANOVA with post-hoc Tukey's test; *** $P < 0.0005$, $P > 0.05$ where
 547 not indicated; $N = 8–10$ SCA6^{84Q/84Q} mice depending on age, 5–9 SCA6^{84Q/+} mice, and 6–9 WT mice,
 548 consult Table 1 for sample size at each age).

549

550 **Figure 2. Increased latency on elevated beam at 7 months in SCA6^{84Q/84Q} mice.**

551 A, schematic of experimental design for elevated beam assay. Two days of training were followed by
 552 two days of testing (D1 and D2 in panels B–E). B–E, latency to cross beam was measured for each
 553 genotype at each age (3, 4, 5, 6, and 7 months) over D1 and D2. SCA6^{84Q/84Q} mice were significantly
 554 slower at traversing the beam at 7 months on D2 for the following diameters: B, 22 mm ($F_{2,17} = 7.36$; P
 555 $= 0.005$) C, 18 mm ($F_{2,17} = 7.46$; $P = 0.005$), D, 15 mm ($F_{2,17} = 4.34$; $P = 0.03$), and E, 12 mm ($F_{2,17} =$
 556 5.27 ; $P = 0.017$), while SCA6^{84Q/+} mice were indistinguishable from WT. * $P < 0.05$, ** $P < 0.01$, *** P
 557 < 0.005 , $P > 0.05$ where not indicated, one-way ANOVA followed by post-hoc Tukey's test; $N = 8–10$
 558 SCA6^{84Q/84Q} mice depending on age, 5–9 SCA6^{84Q/+} mice, and 6–9 WT mice, consult Table 1 for
 559 sample size at each age.

560

561 **Figure 3. Increased footslips on narrow elevated beam at 7 months in SCA6^{84Q/84Q} mice.**

562 *A–D*, the number of mice that display footslips (0 footslips = lightest colour, > 2 footslips = darkest
563 colour, and 1 and 2 footslips graded in between) when crossing beams for 3 genotypes: WT (greyscale)
564 SCA6^{84Q/+} (orange-scale) and SCA6^{84Q/84Q} mice (red-scale); see legend on the right. No differences
565 were seen across genotypes and age for: *A*, 22 mm diameter beam ($F_{2,37} = 0.17$; $P = 0.85$); *B*, 18 mm
566 beam ($F_{2,37} = 1.91$; $P = 0.16$); *C*, 15 mm beam ($F_{2,37} = 0.65$; $P = 0.53$); *D*, a significant increase in the
567 number of footslips was observed for the 12 mm beam at 7 months for SCA6^{84Q/84Q} mice ($F_{2,37} = 4.19$;
568 $P = 0.02$). * $P < 0.05$, $P > 0.05$ where not indicated, one-way ANOVA followed by post-hoc Tukey's
569 test; $N = 8–10$ SCA6^{84Q/84Q} mice depending on age, 5–9 SCA6^{84Q/+} mice, and 6–9 WT mice, consult
570 Table 1 for sample size at each age.

571

572 **Figure 4. Reduced swimming deficits at 7 months in SCA6^{84Q/84Q} mice.**

573 *A*, schematic showing the experimental design for the swimming assay. Mice were trained for 2 days
574 and subsequently tested over 3 days (D1-D3 in panels *B* and *C*). *B*, no significant differences in swim
575 latency were observed for mice across ages and genotypes (Age X Genotype: $F_{8,105} = 1.85$; $p = 0.07$;
576 see Table 1 for N 's). *C*, in contrast to latency, there was an increase in the number of hind-limb kicks
577 performed to cross the tank at 7 months in SCA6^{84Q/84Q} but not SCA6^{84Q/+} compared to WT mice (Age
578 X Genotype X Days: $F_{16,210} = 1.81$; $P = 0.03$). $N = 8–10$ SCA6^{84Q/84Q} mice depending on age, 5–9
579 SCA6^{84Q/+} mice, and 6–9 WT mice, consult Table 1 for sample size at each age. *D*, summary data
580 showing the number of kicks on Day 3 at 7 months old for the different genotypes. * $P < 0.05$ one-way
581 ANOVA followed by Tukey's post-hoc test; $N = 6$ WT, 5 SCA6^{84Q/+}, 9 SCA6^{84Q/84Q}.

582

583 **Figure 5. No abnormalities observed in gait in SCA6^{84Q} mice before or at the onset of motor**
 584 **coordination deficits.**

585 *A*, schematic of painted footprint experiment used to study gait: forelimbs were painted blue and hind
 586 limbs were painted red. *B*, representative footprints from mice in each genotype reveal no significant
 587 differences in gait. (*C–H*) The distance between subsequent limb placements (stride length) at 4, 6, and
 588 7 months were not significantly different across phenotypes for: *C*, left hind limb ($F_{2,63} = 0.14$; $P =$
 589 0.87); *D*, left forelimb ($F_{2,63} = 0.25$; $P = 0.78$); *E*, right hind limb ($F_{2,63} = 0.46$; $P = 0.64$); and, *F*, right
 590 forelimb stride lengths ($F_{2,63} = 0.08$; $P = 0.91$). Likewise, no significant differences were observed for
 591 stance (distance between left and right limb placements) of: *G*, hind limbs ($F_{2,63} = 1.23$; $P = 0.30$); and
 592 *H*, forelimbs ($F_{2,63} = 0.53$; $P = 0.60$) at 4, 6, or 7 months. One-way ANOVA; $N = 8–10$ SCA6^{84Q/84Q}
 593 mice depending on age, 5–9 SCA6^{84Q/+} mice, and 6–9 WT mice, consult Table 1 for sample size at
 594 each age.

595

596 **Figure 6. Disease progression marked by no gait abnormalities, but worsening motor**
 597 **coordination.**

598 *A–F*, gait was examined in aging animals that were 1- and 2-years old to determine if differences in
 599 gait emerged as SCA6 progressed. The stride length at 1 and 2 years were not significantly different
 600 across SCA6^{84Q/84Q} and WT mice for: *A*, left hind limb ($F_{1,27} = 0.08$; $P = 0.77$); *B*, left forelimb ($F_{1,27} =$
 601 0.01 ; $P = 0.90$); *C*, right hind limb ($F_{1,27} = 0.002$; $P = 0.97$); and, *D*, right forelimb stride lengths ($F_{1,27}$
 602 $= 0.10$; $P = 0.76$). Nor were significant differences observed for stance (distance between left and right
 603 limb placements) of: *E*, hind limbs ($F_{1,27} = 0.0001$; $P = 0.99$); and *F*, forelimbs ($F_{1,27} = 0.17$; $P = 0.68$).
 604 *G*, motor coordination abnormalities worsened with age for 1- and 2-year-old mice on Rotarod (1 year,

Ataxia onset prior to neurodegeneration in SCA6

Genotype: $F_{1,30} = 56.01$; $P < 0.0001$; 2 year, Genotype: $F_{1,28} = 33.62$; $P < 0.0001$). *** $P < 0.001$ one-way ANOVA followed by Tukey's post-hoc test; $N = 8$ WT and 8 SCA6^{84Q/84Q} 1-year-old mice; $n = 7$ WT and 8 SCA6^{84Q/84Q} 2-year-old mice.

608

Figure 7. Purkinje cell degeneration is observed long after the onset of motor phenotype at 2 years in SCA6^{84Q/84Q} mice.

A, representative images of calbindin-stained Purkinje cells from 7-month-old WT (left) and SCA6^{84Q/84Q} (right) mouse cerebellar slices. The height of the molecular layer is indicated. Scale bar for both images, 20 μ m. B, density of Purkinje cells in 7-month-old cerebellum is not significantly different in SCA6^{84Q/84Q} compared to WT mice (Genotype: $F_{1,109} = 0.002$, $P = 0.96$). However, reduced Purkinje cell density is observed at 2 years in SCA6^{84Q/84Q} mice (genotype: $F_{1,97} = 18.76$, $P < 0.0001$; right). C, representative images of 2-year-old WT (left) and SCA6^{84Q/84Q} (right) Purkinje cells. Scale bar for both images, 20 μ m. D, no significant different in Purkinje cell molecular layer is observed at 7 months in SCA6^{84Q/84Q} and WT mice ($F_{1,203} = 0.79$, $P = 0.37$; left), while molecular layer thickness is reduced at 2 years in SCA6^{84Q/84Q} mice compared to WT ($F_{1,189} = 33.12$, $P < 0.0001$; right). $N = 3-4$ animals for each genotype at each age; at least 12 mm of Purkinje cell layer was measured for each comparison; one-way ANOVA with post-hoc Tukey's test. *** $P < 0.0001$, ** < 0.01 , * $P < 0.05$, $P > 0.05$ where not indicated.

Figure 8. No loss of striatal neurons in SCA6^{84Q/84Q} mice accompanies the onset of motor coordination deficits at 7 months.

Ataxia onset prior to neurodegeneration in SCA6

625 *A*, representative images of NeuN-stained cells from 7-month-old WT (left) and SCA6^{84Q/84Q} (right)
626 mouse striatum. Scale bar for both images, 20 μ m. *B*, density of striatal cells is not significantly
627 different in SCA6^{84Q/84Q} compared to WT mice at 7 months (Student's *t*-test, *P* = 0.72).

628

Table 1. Sample size for each genotype at each experimental age

Genotype	N for each experimental age						
	3 months	4 months	5 months	6 months	7 months	1 year	2 years
WT	7	9	8	7	6	8	7
SCA6 ^{84Q/+}	6	9	7	8	5	-	-
SCA6 ^{84Q/84Q}	9	9	8	10	9	8	8

Summary of the number of animals (N) for each of three genotypes used at each experimental age (mice were naive at each age without any prior behavioral training).

Table 2. Statistical Table

Figure & Panel	Description	Test	Degrees of freedom	F-Value	P-Value	95% Confidence interval
1 B	Rotarod (3 to 7 months) - Effect of age	ANOVA - Fit model	4, 105	10.6731	<0.0001	-
1 B	Rotarod (3 to 7 months) - Effect of days X age	ANOVA - Fit model	16, 420	4.6269	<0.0001	-
1 B	Rotarod (3 to 7 months) - Effect of genotype X age	ANOVA - Fit model	8, 105	2.2818	0.0271	-
1 B	Rotarod (3 months) - Effect of genotype	One-WAY ANOVA	2,39	2.5509	0.091	-
1 B	Rotarod (4 months) - Effect of genotype	One-WAY ANOVA	2,51	0.2849	0.7533	-
1 B	Rotarod (5 months) - Effect of genotype	One-WAY ANOVA	2,45	1.5495	0.2235	-
1 B	Rotarod (6 months) - Effect of genotype	One-WAY ANOVA	2,53	0.6127	0.5457	-
1 B	Rotarod (7 months) - Effect of genotype	One-WAY ANOVA	2,37	12.1937	<0.0001	-
1 B	Rotarod (7 months) - WT X SCA6 84Q/84Q	Tukey-HSD	-	-	0.0004	[14.17,52.89]
1 B	Rotarod (7 months) - SCA6 84Q/84Q X SCA6 84Q/-	Tukey-HSD	-	-	0.0009	[12.74,53.71]

Ataxia onset prior to neurodegeneration in SCA6

1	B	Rotarod (7 months) - WT X SCA6 84Q/-	Tukey-HSD	-	-	0.9994	[-21.94, 22.54]
2	B	Balance beam latency, 22 mm (3 to 7 months) - Effect of age	ANOVA - Fit model	4, 105	4.7234	0.0026	-
2	B	Balance beam latency, 22 mm (3 to 7 months) - Effect of genotype X age	ANOVA - Fit model	8, 105	2.0755	0.0446	-
2	B	Balance beam latency, 22 mm (3 months) - Effect of genotype	One-WAY ANOVA	2,18	1.8397	0.1875	-
2	B	Balance beam latency, 22 mm (4 months) - Effect of genotype	One-WAY ANOVA	2,24	1.3117	0.288	-
2	B	Balance beam latency, 22 mm (5 months) - Effect of genotype	One-WAY ANOVA	2,21	1.8648	0.1797	-
2	B	Balance beam latency, 22 mm (6 months) - Effect of genotype	One-WAY ANOVA	2,25	0.1779	0.838	-
2	B	Balance beam latency, 22 mm (7 months) - Effect of genotype	One-WAY ANOVA	2,17	7.3589	0.005	-
2	B	Balance beam latency, 22 mm (7 months) - WT X SCA6 84Q/84Q	Tukey-HSD	-	-	0.0101	[0.78,5.88]
2	B	Balance beam latency, 22 mm (7 months) - SCA6 84Q/84Q X SCA6 84Q/-	Tukey-HSD	-	-	0.021	[0.46,5.86]
2	B	Balance beam latency, 22 mm (7 months) - WT X SCA6 84Q/-	Tukey-HSD	-	-	0.987	[-2.76,3.11]
2	C	Balance beam latency, 18 mm (3 to 7 months) - Effect of age	ANOVA - Fit model	4, 105	2.3582	0.0398	-
2	C	Balance beam latency, 18 mm (3 to 7 months) - Effect of genotype X age	ANOVA - Fit model	8, 105	3.0995	0.0035	-
2	C	Balance beam latency, 18 mm (3 months) - Effect of genotype	One-WAY ANOVA	2,18	1.8068	0.1927	-
2	C	Balance beam latency, 18 mm (4 months) - Effect of genotype	One-WAY ANOVA	2,24	0.0071	0.9929	-
2	C	Balance beam latency, 18 mm (5 months) - Effect of genotype	One-WAY ANOVA	2,21	2.0014	0.1601	-
2	C	Balance beam latency, 18 mm (6 months) - Effect of genotype	One-WAY ANOVA	2,25	0.7112	0.5007	-
2	C	Balance beam latency, 18 mm (7 months) - Effect of genotype	One-WAY ANOVA	2,17	7.4618	0.0047	-
2	C	Balance beam latency, 18 mm (7 months) - WT X SCA6 84Q/84Q	Tukey-HSD	-	-	0.0083	[1.67,11.43]
2	C	Balance beam latency, 18 mm (7 months) - SCA6 84Q/84Q X SCA6 84Q/-	Tukey-HSD	-	-	0.0243	[0.73,11.06]
2	C	Balance beam latency, 18 mm (7 months) - WT X SCA6 84Q/-	Tukey-HSD	-	-	0.9519	[-4.95,6.26]
2	D	Balance beam latency, 15 mm (3 to 7 months) - Effect of age	ANOVA - Fit model	4, 105	1.0691	0.3756	-
2	D	Balance beam latency, 15 mm (3 to 7 months) - Effect of genotype X age	ANOVA - Fit model	8, 105	2.0276	0.05	-
2	D	Balance beam latency, 15 mm (3 months) - Effect of genotype	One-WAY ANOVA	2,18	3.1614	0.0666	-

Ataxia onset prior to neurodegeneration in SCA6

2	D	Balance beam latency, 15 mm (4 months) - Effect of genotype	One-WAY ANOVA	2,24	0.5249	0.5982	-
2	D	Balance beam latency, 15 mm (5 months) - Effect of genotype	One-WAY ANOVA	2,21	0.9172	0.4151	-
2	D	Balance beam latency, 15 mm (6 months) - Effect of genotype	One-WAY ANOVA	2,25	0.4909	0.6178	-
2	D	Balance beam latency, 15 mm (7 months) - Effect of genotype	One-WAY ANOVA	2,17	4.3447	0.0299	-
2	D	Balance beam latency, 15 mm (7 months) - WT X SCA6 84Q/84Q	Tukey-HSD	-	-	0.0382	[0.22,8.51]
2	D	Balance beam latency, 15 mm (7 months) - SCA6 84Q/84Q X SCA6 84Q/-	Tukey-HSD	-	-	0.1167	[-0.77,8.00]
2	D	Balance beam latency, 15 mm (7 months) - WT X SCA6 84Q/-	Tukey-HSD	-	-	0.9143	[-4.01,5.51]
2	E	Balance beam latency, 12 mm (3 to 7 months) - Effect of age	ANOVA - Fit model	4, 105	1.7763	0.1391	-
2	E	Balance beam latency, 12 mm (3 to 7 months) - Effect of genotype X age	ANOVA - Fit model	8, 105	2.1864	0.0342	-
2	E	Balance beam latency, 12 mm (3 months) - Effect of genotype	One-WAY ANOVA	2,18	0.4304	0.6568	-
2	E	Balance beam latency, 12 mm (4 months) - Effect of genotype	One-WAY ANOVA	2,24	1.5008	0.2431	-
2	E	Balance beam latency, 12 mm (5 months) - Effect of genotype	One-WAY ANOVA	2,21	0.332	0.7212	-
2	E	Balance beam latency, 12 mm (6 months) - Effect of genotype	One-WAY ANOVA	2,25	0.4932	0.6165	-
2	E	Balance beam latency, 12 mm (7 months) - Effect of genotype	One-WAY ANOVA	2,17	5.2734	0.0165	-
2	E	Balance beam latency, 12 mm (7 months) - WT X SCA6 84Q/84Q	Tukey-HSD	-	-	0.0427	[0.16,10.23]
2	E	Balance beam latency, 12 mm (7 months) - SCA6 84Q/84Q X SCA6 84Q/-	Tukey-HSD	-	-	0.0351	[0.33,9.85]
2	E	Balance beam latency, 12 mm (7 months) - WT X SCA6 84Q/-	Tukey-HSD	-	-	0.9987	[-5.37,5.57]
3	A	Balance beam footslips, 22 mm (3 to 7 months) - Effect of age	ANOVA - Fit model	4, 105	2.1833	0.0759	-
3	A	Balance beam footslips, 22 mm (3 to 7 months) - Effect of genotype X age	ANOVA - Fit model	8, 105	0.5829	0.79	-
3	A	Balance beam footslips, 22 mm (7 months) - Effect of genotype	One-WAY ANOVA	2,37	0.1683	0.8458	-
3	B	Balance beam footslips, 18 mm (3 to 7 months) - Effect of age	ANOVA - Fit model	4, 105	1.589	0.1827	-
3	B	Balance beam footslips, 18 mm (3 to 7 months) - Effect of genotype X age	ANOVA - Fit model	8, 105	0.6673	0.7191	-
3	B	Balance beam footslips, 18 mm (7 months) - Effect of genotype	One-WAY ANOVA	2,37	1.9098	0.1624	-

Ataxia onset prior to neurodegeneration in SCA6

3	C	Balance beam footslips, 15 mm (3 to 7 months) - Effect of age	ANOVA - Fit model	4, 105	2.1859	0.0756	-
3	C	Balance beam footslips, 15 mm (3 to 7 months) - Effect of genotype X age	ANOVA - Fit model	8, 105	0.5983	0.7779	-
3	C	Balance beam footslips, 15 mm (7 months) - Effect of genotype	One-WAY ANOVA	2,37	0.6498	0.528	-
3	D	Balance beam footslips, 12 mm (3 to 7 months) - Effect of age	ANOVA - Fit model	4, 105	2.1259	0.0827	-
3	D	Balance beam footslips, 12 mm (3 to 7 months) - Effect of genotype X age	ANOVA - Fit model	8, 105	2.1089	0.0412	-
3	D	Balance beam footslips, 12 mm (3 months) - Effect of genotype	One-WAY ANOVA	2,39	0.1375	0.8719	-
3	D	Balance beam footslips, 12 mm (4 months) - Effect of genotype	One-WAY ANOVA	2,51	0.2186	0.8044	-
3	D	Balance beam footslips, 12 mm (5 months) - Effect of genotype	One-WAY ANOVA	2,45	1.4268	0.424	-
3	D	Balance beam footslips, 12 mm (6 months) - Effect of genotype	One-WAY ANOVA	2,53	0.7188	0.492	-
3	D	Balance beam footslips, 12 mm (7 months) - Effect of genotype	One-WAY ANOVA	2,37	4.1923	0.0229	-
3	D	Balance beam footslips, 12 mm (7 months) - WT X SCA6 84Q/84Q	Tukey-HSD	-	-	0.0386	[0.05,2.12]
3	D	Balance beam footslips, 12 mm (7 months) - SCA6 84Q/84Q X SCA6 84Q/-	Tukey-HSD	-	-	0.0796	[-0.10,2.10]
3	D	Balance beam footslips, 12 mm (7 months) - WT X SCA6 84Q/-	Tukey-HSD	-	-	0.984	[-1.11,1.27]
4	B	Swimming latency (3 to 7 months) - Effect of age	ANOVA - Fit model	4, 105	1.1257	0.3484	-
4	B	Swimming latency (3 to 7 months) - Effect of genotype	ANOVA - Fit model	2, 105	0.0301	0.9704	-
4	B	Swimming latency (3 to 7 months) - Effect of age X genotype	ANOVA - Fit model	8, 105	1.8585	0.0744	-
4	C	Swimming kicks (3 to 7 months) - Effect of age	ANOVA - Fit model	4, 105	1.8924	0.1421	-
4	C	Swimming kicks (3 to 7 months) - Effect of genotype	ANOVA - Fit model	2, 105	1.4178	0.2468	-
4	C	Swimming kicks (3 to 7 months) - Effect of age X genotype	ANOVA - Fit model	8, 105	1.6343	0.1238	-
4	C	Swimming kicks (3 to 7 months) - Effect of age X genotype X days	ANOVA - Fit model	16, 210	1.812	0.0312	-
4	D	Swimming kicks 7 months (Day 3 of testing) - SCA6 84Q/84Q X WT	Tukey-HSD	-	-	0.0375	[0.07, 6.71]
4	D	Swimming kicks 7 months (Day 3 of testing) - SCA6 84Q/84Q X SCA6 84Q/-	Tukey-HSD	-	-	0.0439	[0.09, 6.78]

Ataxia onset prior to neurodegeneration in SCA6

4	D	Swimming kicks 7 months (Day 3 of testing) - SCA6 84Q/- X WT	Tukey-HSD	-	-	>1	[-3.68, 3.94]
5	C	Stride left hindlimb (4 to 7 months) - Effect of genotype	ANOVA- Fit model	2,63	0.1432	0.8741	-
5	C	Stride left hindlimb (4 months) - Effect of genotype	One-WAY ANOVA	2,21	0.1633	0.8504	-
5	C	Stride left hindlimb (6 months) - Effect of genotype	One-WAY ANOVA	2,25	0.0946	0.91	-
5	C	Stride left hindlimb (7 months) - Effect of genotype	One-WAY ANOVA	2,17	0.3729	0.6942	-
5	D	Stride right hindlimb (4 to 7 months) - Effect of genotype	ANOVA- Fit model	2,63	0.4552	0.6381	-
5	D	Stride right hindlimb (4 months) - Effect of genotype	One-WAY ANOVA	2,21	0.1701	0.8447	-
5	D	Stride right hindlimb (6 months) - Effect of genotype	One-WAY ANOVA	2,25	0.1729	0.8422	-
5	D	Stride right hindlimb (7 months) - Effect of genotype	One-WAY ANOVA	2,17	0.0981	0.9071	-
5	E	Stance hindlimb (4 to 7 months) - Effect of genotype	ANOVA- Fit model	2,63	1.2341	0.2981	-
5	E	Stance hindlimb (4 months) - Effect of genotype	One-WAY ANOVA	2,21	0.4725	0.6299	-
5	E	Stance hindlimb (6 months) - Effect of genotype	One-WAY ANOVA	2,25	0.0238	0.9765	-
5	E		One-WAY ANOVA	2,17	0.5018	0.6141	-
5	F	Stride left forelimb (4 to 7 months) - Effect of genotype	ANOVA- Fit model	2,63	0.2511	0.7804	
5	F	Stride left forelimb (4 months) - Effect of genotype	One-WAY ANOVA	2,21	0.3767	0.6907	-
5	F	Stride left forelimb (6 months) - Effect of genotype	One-WAY ANOVA	2,25	0.5051	0.6094	-
5	F	Stride left forelimb (7 months) - Effect of genotype	One-WAY ANOVA	2,17	0.4583	0.6399	-
5	G	Stride right forelimb (4 to 7 months) - Effect of genotype	ANOVA- Fit model	2,63	0.0758	0.9124	-
5	G	Stride right forelimb (4 months) - Effect of genotype	One-WAY ANOVA	2,21	0.2384	0.79	-
5	G	Stride right forelimb (6 months) - Effect of genotype	One-WAY ANOVA	2,25	0.2074	0.7653	-
5	G	Stride right forelimb (7 months) - Effect of genotype	One-WAY ANOVA	2,17	0.2588	0.775	-
5	H	Stance forelimb (4 to 7 months) - Effect of genotype	ANOVA- Fit model	2,63	0.5312	0.6042	-
5	H	Stance forelimb (4 months) - Effect of genotype	One-WAY ANOVA	2,21	0.3596	0.7022	-
5	H	Stance forelimb (6 months) - Effect of genotype	One-WAY ANOVA	2,25	1.2299	0.3094	-
5	H	Stance forelimb (7 months) - Effect of genotype	One-WAY ANOVA	2,17	0.5272	0.5996	-
6	A	Stride left hindlimb (1-2 year) - Effect of genotype	ANOVA- Fit model	1,27	0.08	0.7654	-
6	A	Stride left hindlimb (1 year) - Effect of genotype	One-WAY ANOVA	1,14	0.4616	0.5079	-

Ataxia onset prior to neurodegeneration in SCA6

6	A	Stride left hindlimb (2 year) - Effect of genotype	One-WAY ANOVA	1,13	0.1893	0.6707	-
6	B	Stride right hindlimb (1-2 year) - Effect of genotype	ANOVA- Fit model	1,27	0.002	0.9704	-
6	B	Stride right hindlimb (1 year) - Effect of genotype	One-WAY ANOVA	1,14	0.2275	0.6407	-
6	B	Stride right hindlimb (2 year) - Effect of genotype	One-WAY ANOVA	1,13	0.3613	0.5581	-
6	C	Stance hindlimb (1-2 year) - Effect of genotype	ANOVA- Fit model	1,27	0.0001	0.9871	-
6	C	Stance hindlimb (1 year) - Effect of genotype	One-WAY ANOVA	1,14	0.5178	0.4836	-
6	C	Stance hindlimb (2 year) - Effect of genotype	One-WAY ANOVA	1,13	0.5202	0.4835	-
6	D	Stride left forelimb (1-2 year) - Effect of genotype	ANOVA- Fit model	1,27	0.0117	0.9045	-
6	D	Stride left forelimb (1 year) - Effect of genotype	One-WAY ANOVA	1,14	0	1	-
6	D	Stride left forelimb (2 year) - Effect of genotype	One-WAY ANOVA	1,13	0.0453	0.8348	-
6	E	Stride right forelimb (1-2 year) - Effect of genotype	ANOVA- Fit model	1,27	0.1049	0.7559	-
6	E	Stride right forelimb (1 year) - Effect of genotype	One-WAY ANOVA	1,14	0.0692	0.7963	-
6	E	Stride right forelimb (2 year) - Effect of genotype	One-WAY ANOVA	1,13	0.0308	0.8635	-
6	F	Stance forelimb (1-2 year) - Effect of genotype	ANOVA- Fit model	1,27	0.1742	0.6841	-
6	F	Stance forelimb (1 year) - Effect of genotype	One-WAY ANOVA	1,14	0.5657	0.4644	-
6	F	Stance forelimb (2 year) - Effect of genotype	One-WAY ANOVA	1,13	0.0059	0.94	-
6	E	Rotarod (1 year) - Effect of genotype	One-WAY ANOVA	1,30	56.012	<0.0001	-
6	E	Rotarod (1 year) - WT X SCA6 84Q/84Q	Tukey-HSD	-	-	<0.0001	[44.07, 77.15]
6	E	Rotarod (2 year) - Effect of genotype	One-WAY ANOVA	1,28	33.6153	<0.0001	-
6	E	Rotarod (2 year) - WT X SCA6 84Q/84Q	Tukey-HSD	-	-	<0.0001	[19.35, 40.48]
7	B	Purkinje cell count/100 um (7 months) - Effect of genotype	One-WAY ANOVA	1, 109	0.0023	0.9616	-
7	B	Purkinje cell count/100 um (2 year) - Effect of genotype	One-WAY ANOVA	1, 97	18.7953	<0.0001	-
7	B	Purkinje cell count/100 um (2 year) - WT X SCA6 84Q/84Q	One-WAY ANOVA	-	-	<0.0001	[0.58, 1.57]
7	D	Molecular layer length (7 months) - Effect of genotype	One-WAY ANOVA	1, 203	0.7918	0.3746	-
7	D	Molecular layer length (2 year) - Effect of genotype	One-WAY ANOVA	1, 189	33.1151	<0.0001	-
7	D	Molecular layer length (2 year) - WT X SCA6 84Q/84Q	One-WAY ANOVA	-	-	<0.0001	[27.35, 55.87]

635

Ataxia onset prior to neurodegeneration in SCA6

636

637 **Multimedia**

638 *Movie 1* Rotarod assay

639 SCA6^{84Q/84Q} mouse (right chamber) spends less time on an accelerating rotating rod compared to the
640 litter-matched WT control mouse (left chamber) at 7 months.

641

642 *Movie 2* Sample Rotarod assay (entire trial at high speed).

643 SCA6^{84Q/84Q} mouse (right chamber) spends less time on an accelerating rotating rod compared to the
644 litter-matched WT control mouse (left chamber) at 7 months. Mice are the same as in Movie 1, but the
645 entire trial is shown, at 4X speed.

646

647 *Movie 3* Elevated beam assay

648 A 7-month-old WT mouse crosses an elevated beam.

649

650 *Movie 4* Elevated beam assay illustrating footslips (in slow motion)

651 An SCA6^{84Q/84Q} mouse slipping 3 times on the elevated beam assay, shown in slow motion.

652

653 *Movie 5* Swimming assay (top view)

Ataxia onset prior to neurodegeneration in SCA6

654 A 7-month-old SCA6^{84Q/84Q} mouse swims across the tank.

655

656 *Movie 6* Swimming assay – SCA6^{84Q/84Q} mouse (side view).

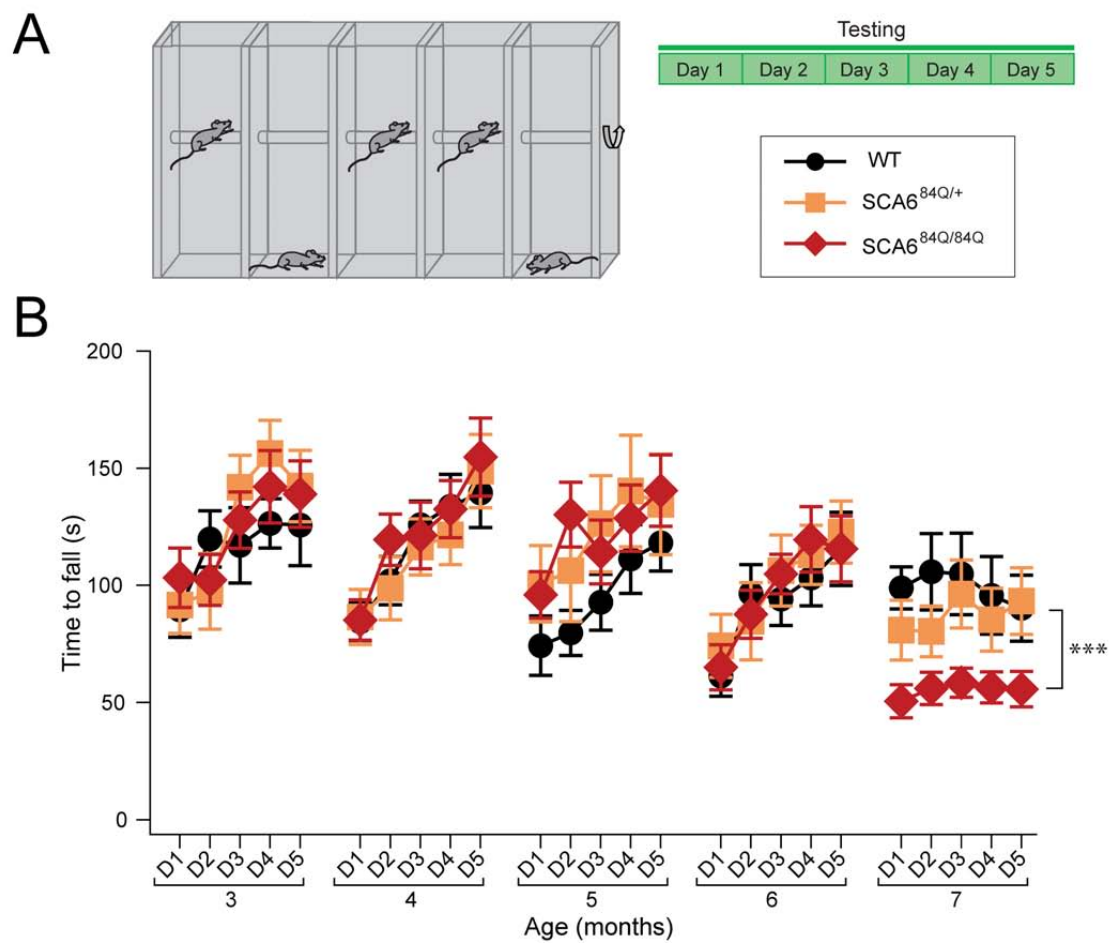
657 A 7-month-old SCA6^{84Q/84Q} mouse swims across the tank. Asterisks indicate right hind limb kicks; 19
658 kicks were counted.

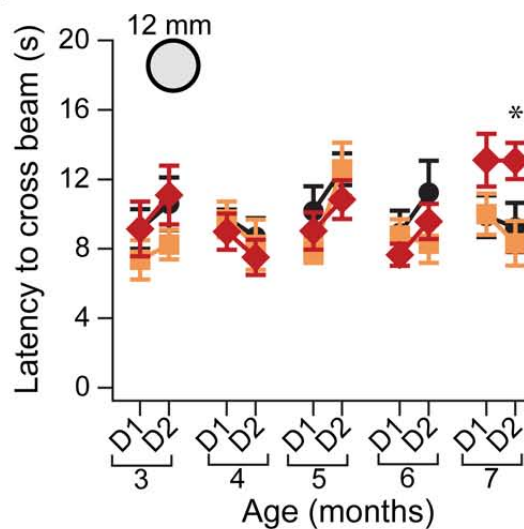
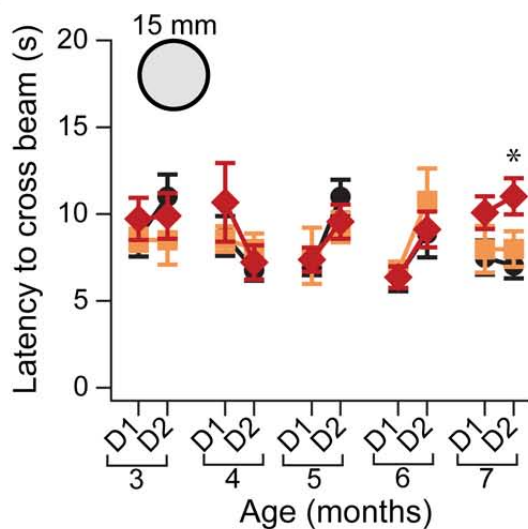
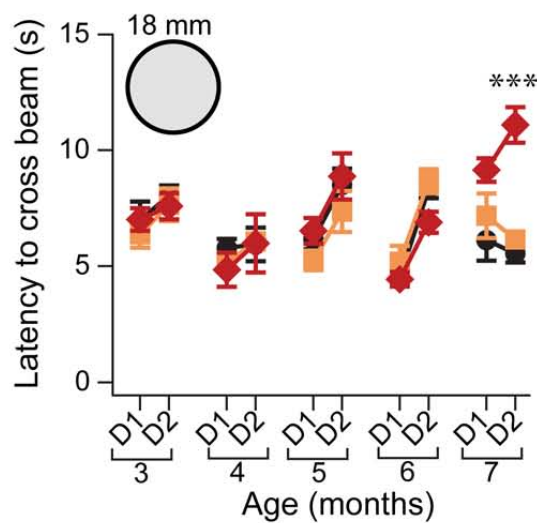
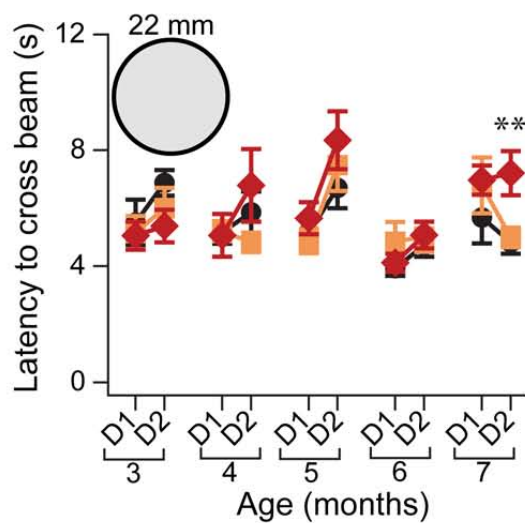
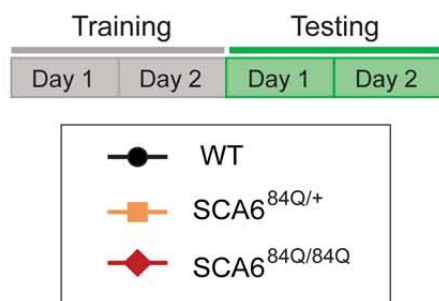
659

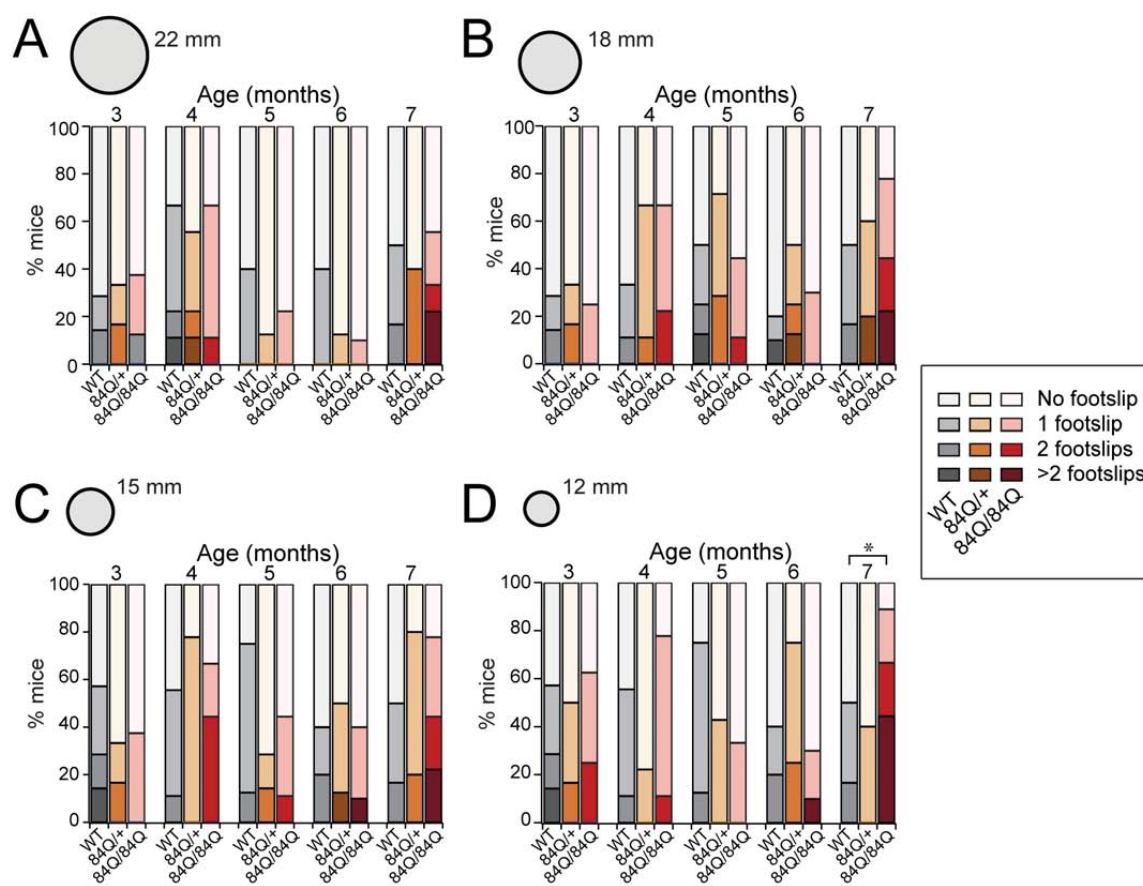
660 *Movie 7* Swimming assay – WT mouse (side view).

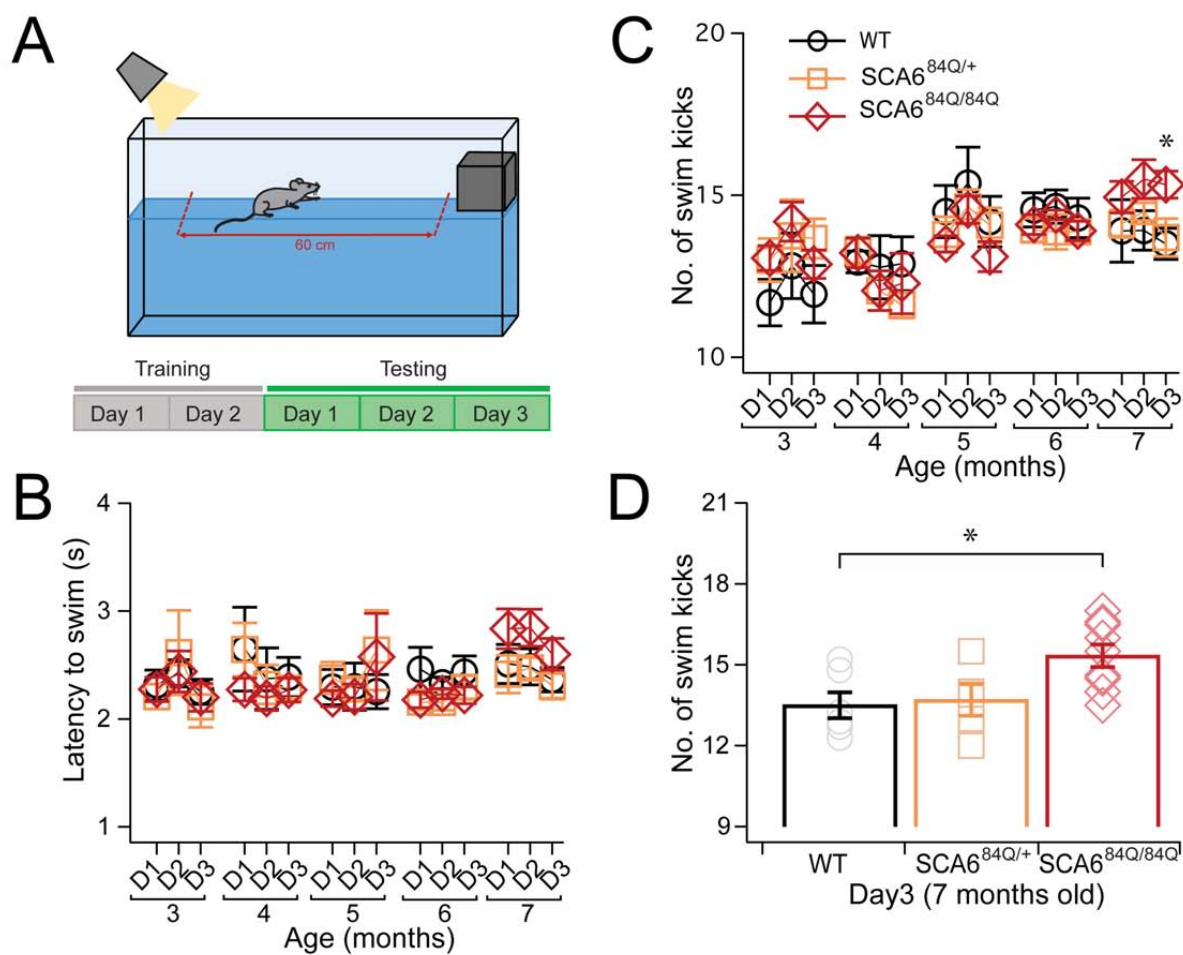
661 A 7-month-old WT mouse swims across the tank. Asterisks indicate right hind limb kicks; 15 kicks
662 were counted.

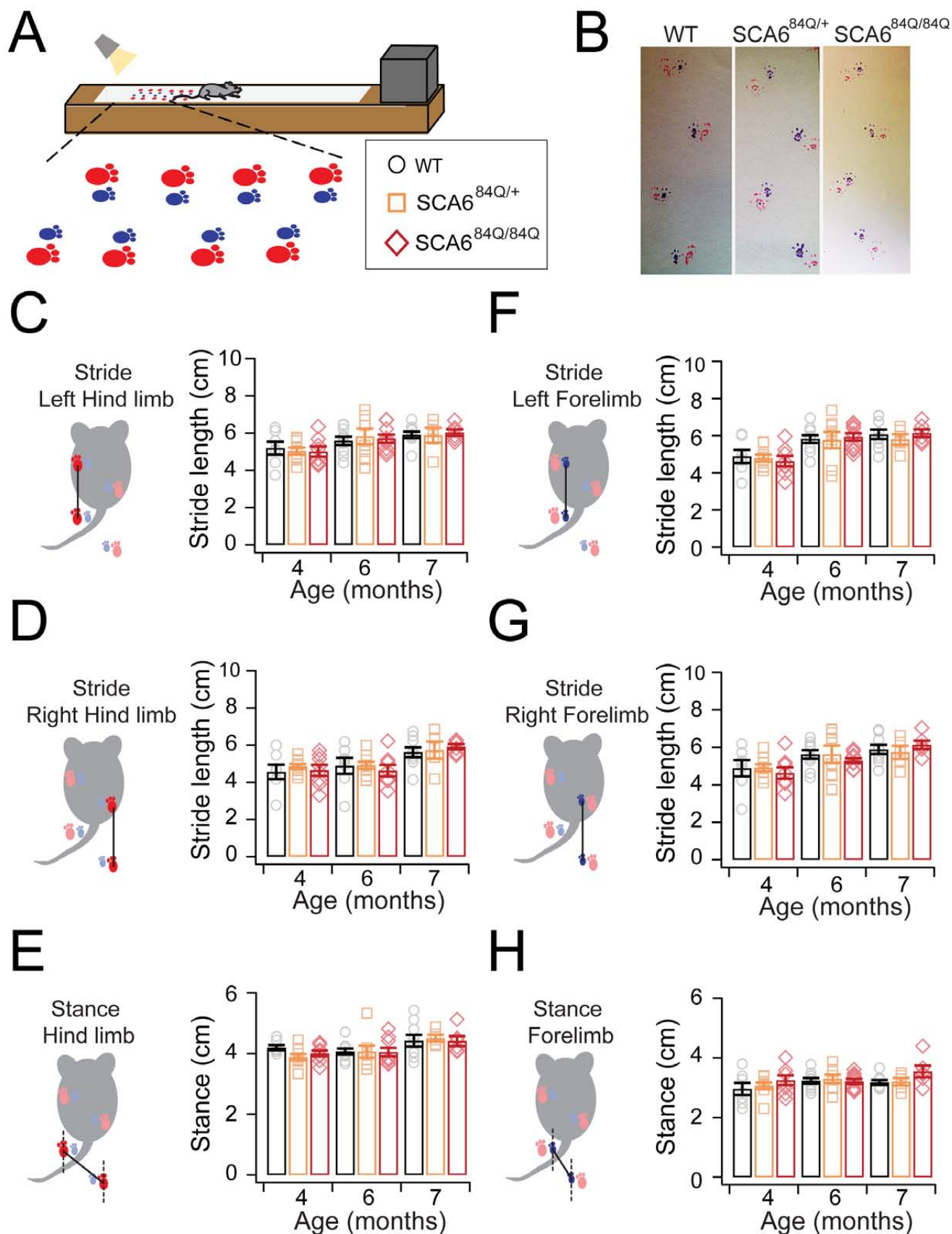
663

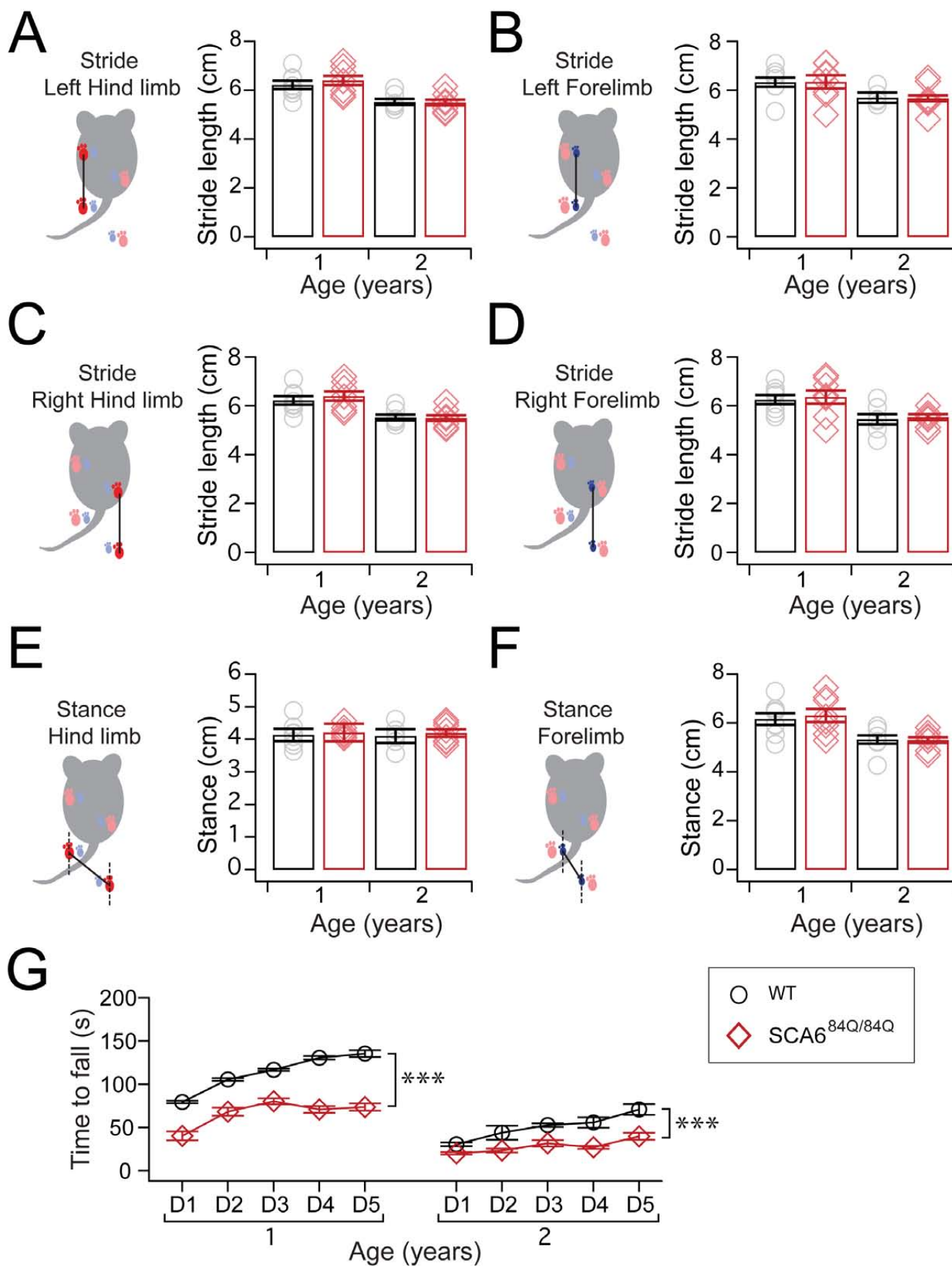


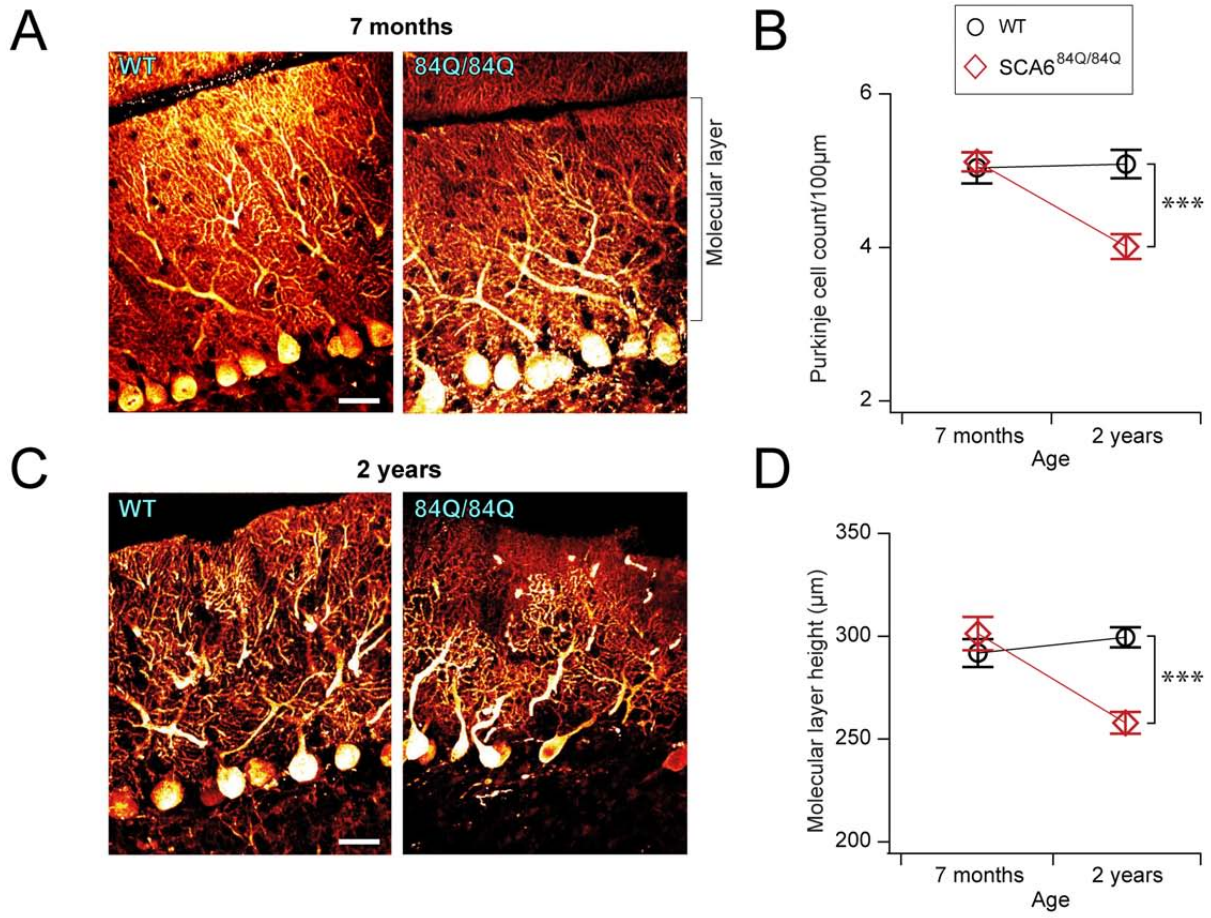




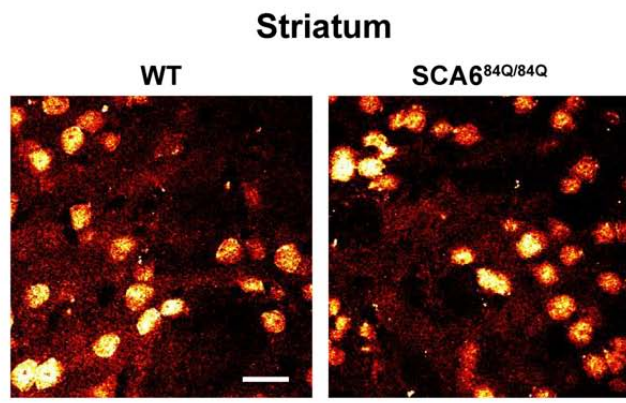








A



B

